university of groningen

Investigating the possibility of using hemin as a catalyst for metabolism of drug compounds to facilitate drug development and establishment of viable drug candidates in an efficient and cost-effective manner

Name:	Sina Nikbakht
Student number:	S4132696
Date:	08-11-2022
Coordinator:	Jennifer Le

1. Abstract

In order to identify novel viable drug candidates in pre-clinical trials, new methods need to be found to make identification easier, cheaper, and more environmentally friendly, while reducing the complexity of research. This study focused on investigating whether heme can be used as a catalyst for the metabolism of substrates instead of CYP, using a simple experimental cyclic voltammetry setup in order to prevent complexity of the study. Hemin was found to be reduced at -0.361 V vs Ag/AgCl in saturated KCl. Pyridine was added to hemin, as binding of pyridine to hemin causes the molecule to become a penta-coordinated molecule, allowing the molecule to transform into a high-spin molecule after reduction, which is important for binding oxygen in its catalytic cycle. Adding pyridine caused hemin's reduction potential to shift towards a slightly more positive potential of -0.322 V, suggesting successful binding of pyridine to hemin. Two substrates were tested to evaluate the ability of hemin to perform the hydroxylation reaction, which is a common reaction pathway performed by cytochrome P450 in phase 1 metabolism. Fenbendazole showed reactivity in voltammograms after testing, but acetyl salicylic acid did not show reactivity, thus it is suggested that hemin can act as a catalyst for metabolism, but might not be suitable for all drugs.

2. Introduction

Drug development is one of the most important branches in research worldwide. Over the years, life expectancy has become much longer than it used to be, and this is partly due to the efforts of those involved in the research and development of novel drugs to be used in the healthcare industry. With increasing lifespan, new diseases are discovered for which new drugs need to be developed. But drug development can be very time and money consuming, which may be necessary for improvement of human life and prevention of misery and death caused by those diseases, but which oftentimes has a negative effect on our planet, as drug development is often performed in an environmentally unfriendly manner. In order to ensure not only improvement of human life, but also the survival of our planet, new methods must be found to facilitate drug development in more effective, cheaper, and environmentally friendly manners to establish viable drug candidates prior to costly clinical trials.

An important part of drug research during its development is the metabolites that are produced when drugs are broken down by the human body, often though specialized enzymatic systems. Metabolism in the human body has three phases: [1] phase 1 metabolism (modification), where drugs are enzymatically transferred into more polar compounds, mainly consisting of, but not limited to, oxidation of substrates by cytochrome P450 (CYP), [2] phase 2 metabolism (conjugation), where these activated or inactivated metabolites are conjugated with compounds in order to make the metabolite more water soluble to facilitate excretion in the bile and/or urine, [3] phase 3 metabolism, where formed metabolites, in case they cannot cross the membrane unassisted, are transported over the membrane to facilitate excretion by either the ATP-binding cassette (ABC) or the solute-carrier (SLC) transporters. (1,2) It is very important to study drug metabolites in order to find out whether they are active or inactive (as a previously inactive drug can become active after metabolism, also called a prodrug), or whether they can possibly induce toxic effects and if so in what quantities the drug can be safely used.

CYP-enzymes are involved in the catalysis of metabolism of more than 75% of FDA-approved drugs (3), and it is very interesting to use these enzymes in research for finding novel viable drug candidates. The metabolism of molecules by CYP happens through oxidation via a catalytic cycle. This catalytic cycle is shown in figure 1, and consists of eight steps. The cycle starts with the introduction of a substrate, which results in an H_2O molecule leaving from heme in order to make room for the substrate [1]. After water has left the binding pocket of hemin, Fe^{3+} is reduced into Fe^{2+} [2], followed by the binding of an oxygen molecule to this Fe^{2+} [3]. Next, the iron-bound oxygen is reduced [4], allowing this O_2^- to become protonated, forming peroxide [5], followed by a final protonation, resulting in another H_2O molecule leaving [6].

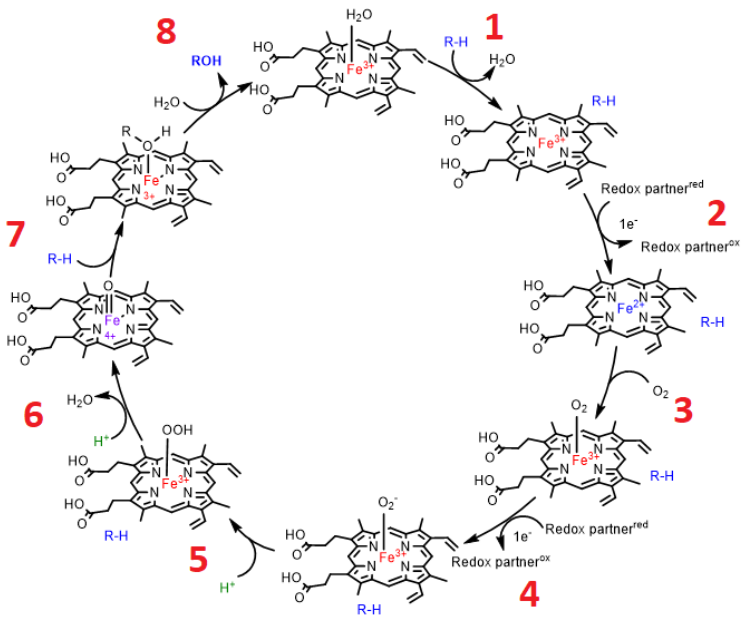

Figure 1: The catalytic cycle of CYP. Note that a cysteine is bound to the iron ion, but has been omitted from the figure for clarity

We now have a ferryl-oxygen ion, or oxo-iron(IV) porphyrin. This oxo-iron(IV) porphyrin catalyzes oxidation of the substrate through a hydroxylation reaction involving a hydrogen atom abstraction from the substrate C-H bond, forming a carbon-centered radical. As this formed radical is unstable, it rebounds to ferryl-hydroxide, forming the oxidized substrate and reducing the ferryl iron back to the ferric resting state [7]. The formed R-O-H complex is finally removed by the introduction of an H_2O molecule, reforming the starting molecule, ready to undergo the catalytic cycle [8]. A few key features in the catalytic cycle of heme are steps 2 and 4, for which redox partners are necessary to facilitate the reduction of Fe^{3+} and O_2, and without these redox partners, the catalytic cycle cannot occur. However, the use of redox partners is often unwanted as this severely increases the system's complexity, making it much harder to perform. In order to keep the system as simple as possible, cyclic voltammetry (CV) can be used. Cyclic voltammetry is an electroanalytical technique used to determine reactivity of analytes and their specific redox potentials. A simple CV setup can be seen in figure 2, where electrodes connected to a potentiostat have been introduced into an electrochemical cell containing the analyte solution. Each electrode has a function: [1] the working electrode donates an electron to or withdraws an electron from the analyte in solution, [2] for each electron donated or withdrawn by the electrode, the counter electrode does the opposite to the solution containing supporting electrolyte in order to keep the charge balance, and [3] the reference electrode measures the solution potential.

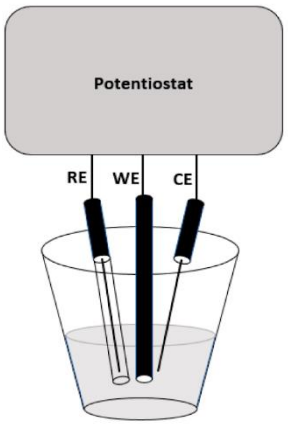

Figure 2: The cyclic voltammetry setup

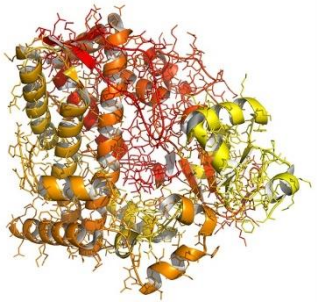

Figure 3: The structure of Cytochrome P450 (18)

The structure of CYP can be seen in figure 3: CYP is a very big protein, and its active site is not easily accessed, making it hard to use in research. This brings us to the interest in using hemin as a catalyst. Heme is the active site in the CYP enzyme, where substrate is metabolized through oxidation by the iron-(IV)-bound oxygen in the center of the heme molecule. Using hemin compared to using the whole enzyme is beneficial due to a couple of reasons: [1] heme is much cheaper than CYP, which can save a lot of money when doing research for extended time periods, [2] CYP is a very large molecule, and it might be more beneficial to use the enzyme without the protein scaffold, as the binding site may be too buried for efficient electron transfer to the electrode. Thus, removing this protein scaffold allows interfacial electron transfer for hemin, but at the cost of specificity.

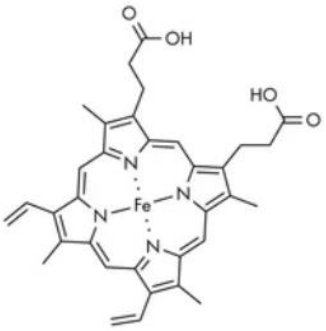

Figure 4: The structure of heme, the active site of CYP. Note that Cysteine is also bound to the iron ion in the center, but is not shown here for clarity (18)

The structure of hemin can be seen in figure 4. Heme is made up of four pyrroles linked together by a methylene bridge, holding an iron-ion in the center. Each pyrrole group holds one methyl group. Heme also has 2 carboxyl groups. Finally, heme in the CYP enzyme has a cysteine bound in the axial position, making it penta-coordinated molecule. This axial-bound ligand is important, as the reduction of Fe^{3+} into Fe^{2+} in the catalytic cycle causes the transition of this penta-coordinated molecule from a low-spin into a high spin molecule, making it a strong oxygen binder.

The purpose of this project is to investigate whether hemin can be used as a catalyst for the metabolism of drugs in a simple, cheap, and effective method by mimicking in-vivo metabolism of substrates using a cyclic voltammetry setup to identify viable drug candidates for further research. Hemin was used during experiments. Hemin is a heme molecule with a chloride ion bound to the axial position instead of cysteine. To mimic the in-vivo metabolism, pyridine was added which can bind to the axial position, forming the penta-coordinated molecule. The investigation of heme as a catalyst is done by first performing characterizing experiments to determine the reactivity and redox potential of hemin, before adding substrates and testing for the formation of metabolites. The substrates investigated were fenbendazole and acetyl salicylic acid (ASA). The structures of these substrates can be seen in figure 5.

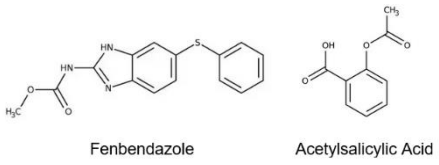

Figure 5: The structures of fenbendazole and acetyl salicylic acid

3. Materials and Methods

3.1 Preparing the electrodes

A three-electrode system was used consisting of a glassy carbon (GC) working electrode (ALS, 1.6 mm diameter), a GC counter electrode (ALS, 3.0 mm diameter) and an Ag/AgCl reference electrode containing saturated KCl solution (4.0 M). As an Ag/AgCl reference electrode was used, all measured potentials are noted in V vs. Ag/AgCl in saturated KCl. To determine the potential in V vs the normal hydrogen electrode (NHE), the following formula can be used: $E_{NHE} = E_{Ag/AgCl} + 0.197$ (4).

The working and counter electrodes were polished using 0.3 alumina on a polishing pad by moving in figure eights 100 times per direction, which amounted to approximately 1:30 minute per direction. Electrodes were washed with UP water to remove any alumina, and finally, the electrodes were sonicated in a water bath containing UP water for 1 minute. Electrodes were reprepared between CV experiments wherever necessary.

3.2 Preparing blank solution and potassium ferricyanide solution

To get familiar with CV, experiments were performed where the one-electron transfer of ferricyanide to ferrocyanide in CV was used as a benchmark to compare to studies with hemin. The concentration for the blank solution was 0.1 M KCl in UP water. Due to the desired reproducibility, experiments with ferricyanide were prepared and performed three separate times. The concentration for the potassium ferricyanide solutions were 5,0285E-03 M, 5,0243E-03 M, and 5,0206E-03 M in 0.1 M KCl. The blank solution was prepared by dissolving 0.75 g KCl in 100 mL UP water to get a 0.1 M KCl solution. The potassium ferricyanide solution was made three times by dissolving 82.78 mg, 82.71 mg, and 82.65 mg potassium ferricyanide in fresh 0.1 M KCl each time.

3.3 Preparation of hemin experiment solutions

For this experiment, all hemin solutions prepared were adapted from (5). Four different solutions were prepared: [1] buffer solution, [2] buffer and pyridine solution, [3] buffer and hemin (iron protoporphyrin IX, EMD Millipore Corp, Sigma Aldrich) solution, and [4] buffer, hemin, and pyridine solution. 200 mL of buffer solution was prepared by adding 1.58 g Tris (0.1 M) (tris (hydroxymethyl) aminomethane) and 1.70 g $NaNO_3$ (0.1 M) to UP water, followed by adding 3 M NaOH until the pH reached approximately 8.000, with actual pH measured being 7.992. 8 g (4% solution) of sodium dodecyl sulfate (SDS, surfactant) was added to the solution and UP water was added to bring up the volume to 200 mL. The solution was heated for 30 minutes at 50 °C. This buffer solution was then used as solvent for the other solutions. The hemin solution contained 205.08 mg hemin ($8{,}9868 * 10^{-3}$ M),

and the hemin/pyridine solution contained 205.37 mg hemin ($8.9996*10^{-3}$ M) and 24.5 µL 99.9% pyridine (hemin:pyridine 1:1).

3.4 Cyclic voltammetry scans with ferricyanide

An electrochemical cell was filled with 5 mL of solution. A Potentiostat (Autolab) connected to a computer was used for the CV scans using the NOVA 1.10 program. Working, counter and reference electrodes were attached to the potentiostat, and submerged into the solution inside of the electrochemical cell. The solution inside the electrochemical cell was sparged where necessary in the experiments. Before performing each scan, a waiting period of 2 minutes was maintained to allow the solution to equilibrate with the electrodes, except in cases where the solution was sparged, as the sparging step also serves as both a mixing and equilibrating step. Two CV experiments containing only blank solution were performed before each sample scan and voltammograms were checked for matching overlay to confirm if the GC electrode was properly prepared. The scan rates used in this experiment were 0.025, 0.050, 0.075, 0.100, 0.200, 0.500 V/s. CVs were run in triplicate, and each CV contained three cycles, with a starting potential of 0 V, up to 0.600 V, down to -0.100 V, and back to 0 V. The data from this scan rate study from NOVA was analyzed in Microsoft Excel. For each scan, the third cycle of the CV was used in data analysis to plot I_P against $\sqrt{v}$ and to determine the diffusion coefficient. According to the Randles-Sevcik equation, I_P at 25 °C is given by the formula $I_P = k * n^{3/2} * A * D^{1/2} * C * v^{1/2}$, where k is a constant $2.72*10^5$, n is the number of electrons transferred in moles, A is the surface area of the working electrode in cm^2, D is the diffusion coefficient, C is the concentration in M, and v is the scan rate. The equation shows that, when scan rate increases, I_P will also increase. The average diffusion coefficient of the 6 scan rates used was calculated with the following formula, derived from the Randles-Sevcik equation: $D = (Slope / (k * n * A * C))^2$. The surface area, 0.0201 cm^2, was calculated using the formula $A = r^2 * \pi$, where r is the radius of the electrode.

3.5 Cyclic voltammetry experiments with hemin

Since hemin was not soluble in water, even under basic conditions (5), surfactant was used to facilitate solubility of hemin via a procedure that proposes that hemin can be encapsulated in micelles using SDS and tetramethylammonium bromide (TMAB) (5). During the experiment, a deviation of the procedure from (5) led to using SDS only instead of in combination with TMAB. To learn more about the way hemin behaves under electrochemical conditions with surfactant, multiple experiments were performed. To find out whether peaks in the CV represented oxygen reduction or reduction and oxidation of the iron ion of hemin, CVs of just the first blank solution were performed where the solution was not sparged, sparged with argon for 5 minutes, then sparged with argon for 20 minutes, and finally aerated with compressed air for 5 minutes to observe the effect of the presence of oxygen in the CV. For the rest of the experiments, all solutions were sparged with argon for 20 minutes to remove any oxygen present in the solution before performing the CV scans.

A scan rate study was performed in order to show whether there is a linear relation between peak current (I_P) and the square root of the scan rate, $\sqrt{v}$. For this scan rate study, the same conditions were used as for ferricyanide, with only two changes. The first change was in scan rate, where an additional scan rate of 1.000 V/s was performed, so scan rates ranged from 0.025 to 1.000 V/s, and studies were performed for both hemin- and hemin/pyridine solutions. The second change was in potential range. The potential range started from 0 V, up to 0.600 V, down to -1.000 V, and back to 0 V for the hemin experiments. The blank CV was performed twice and checked for overlapping voltammograms. If the voltammograms overlapped, there was no need to repolish the electrode, as overlapping voltammograms indicate that the electrodes are properly prepared.

A concentration study was performed with three concentrations: 3-, 6-, and 9 mM 1:1 hemin:pyridine to see the effect of differing concentrations on I_P and E_P.

3.6 Cyclic voltammetry experiments with substrates

Two substrates were used to test for metabolite formation: fenbendazole and ASA, in two different concentrations, added to the buffer solution containing 0.5 mM 1:1 hemin:pyridine. Fenbendazole was added in concentrations of 9.97 mM and 19.98 mM, while ASA was added in concentrations of 10.18 mM and 20.10 mM.

3.7 Statistical analyses

SPSS was used to perform a test for linear regression for I_p vs √v, along with a scatter plot and residuals plot to see whether the model for linear regression fit the data.

4. Results and Discussion

4.1 Cyclic voltammetry experiments with ferricyanide

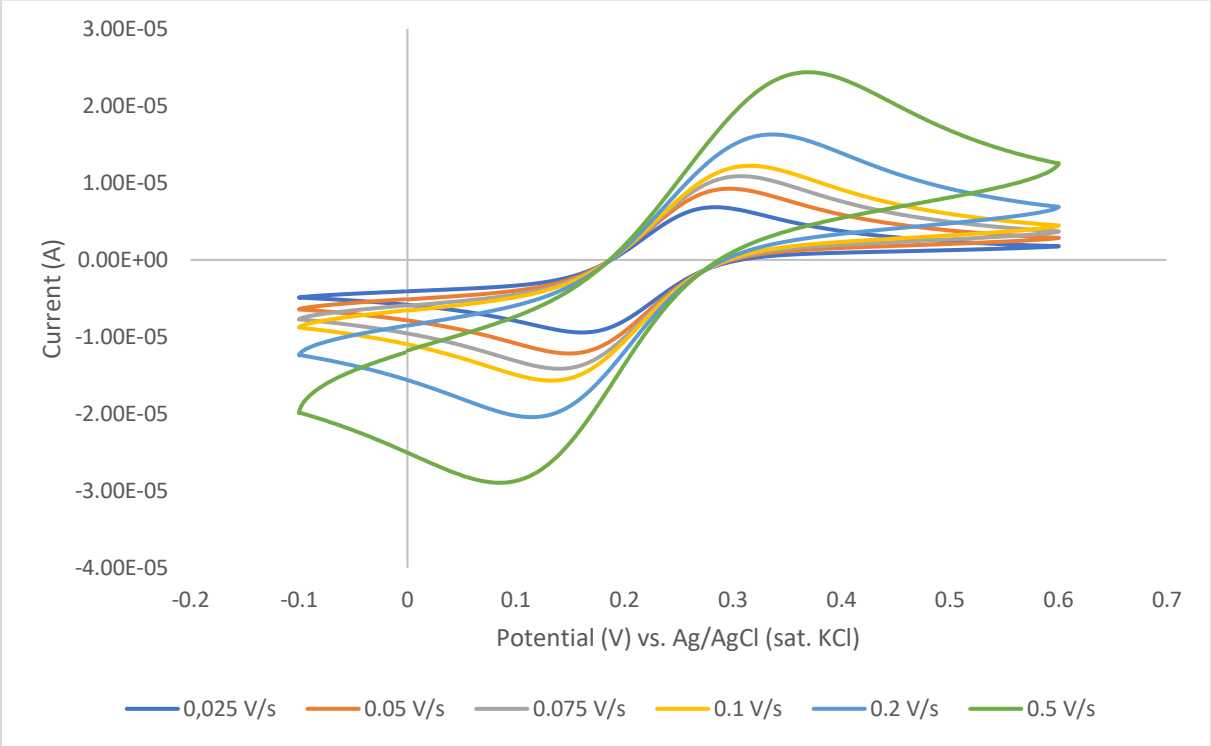

Figure 6: A representative voltammogram showing the relation between IP and v

The voltammogram shows I_P increasing as √v increases. The voltammogram also shows a shift in peak potential, E_P, where E_P shifts to more positive potentials as scan rate increases: there is an increase in peak-to-peak separation. The legend shows which cyclic voltammogram belongs to which scan rate.

As expected, when the scan rate increases, I_P becomes larger. This relationship between I_P and v can be seen in the Randles-Sevcik equation. However, the shift in E_P is unexpected, as this indicates electrochemical irreversibility, or a slow rate of electron transfer (6)*, while this ferricyanide/ferrocyanide system is supposed to be electrochemically reversible, or have a fast rate of electron transfer* (7)*. Note that slow and fast do not indicate the speed of electron transfer, but rather how easy it is for electron transfer to occur, with fast electron transfer meaning that it occurs more easily and thus frequently whenever an analyte molecule approaches the electrode* (6)*. In case of electrochemical reversibility, the E_P should not change with scan rate, and the two peaks of the wave*

should be about 60 mV apart (6). *Table 1 shows the actual peak-to-peak separation of the waves, which are much larger than 60 mV, and* E_P *keeps increasing with increasing scan rates. This increasing* E_P *might indicate that the solution resistance has been improperly compensated* (6). *Solution resistance is often compensated by the potentiostat* (6). *Due to some remaining, uncompensated resistance (*R_U*), the potential recorded by the potentiostat may be inaccurate; this phenomenon is called ohmic drop, and is indicated by increased peak-to-peak separation for a known electrochemically reversible redox event, as is the case in this system* (7). *This* R_U *can be diminished by lessening the distance between WE and RE, or by increasing the solution conductivity with higher electrolyte concentrations, but the solution resistance should never be fully compensated, as this resistance is necessary for proper collection of the CV* (6,7). *Usually, a solution resistance of 2 – 40 Ω is acceptable* (6). *When peak-to-peak separation shifts with scan rate in a system, we can say that the system is electrochemically quasi-reversible* (7).

Table 1: peak-to-peak separation (ΔEP) of the cyclic voltammograms shown in figure 6

Scan rate v/s	0.025	0.05	0.075	0.1	0.2	0.5
I_P min (V)	0,161133	0,150147	0,141602	0,131836	0,114746	0,084229
I_P max (V)	0,283203	0,297852	0,307617	0,314941	0,336914	0,368652
ΔE_P (mV)	122.07	147.71	166.02	183.11	222.17	284.42

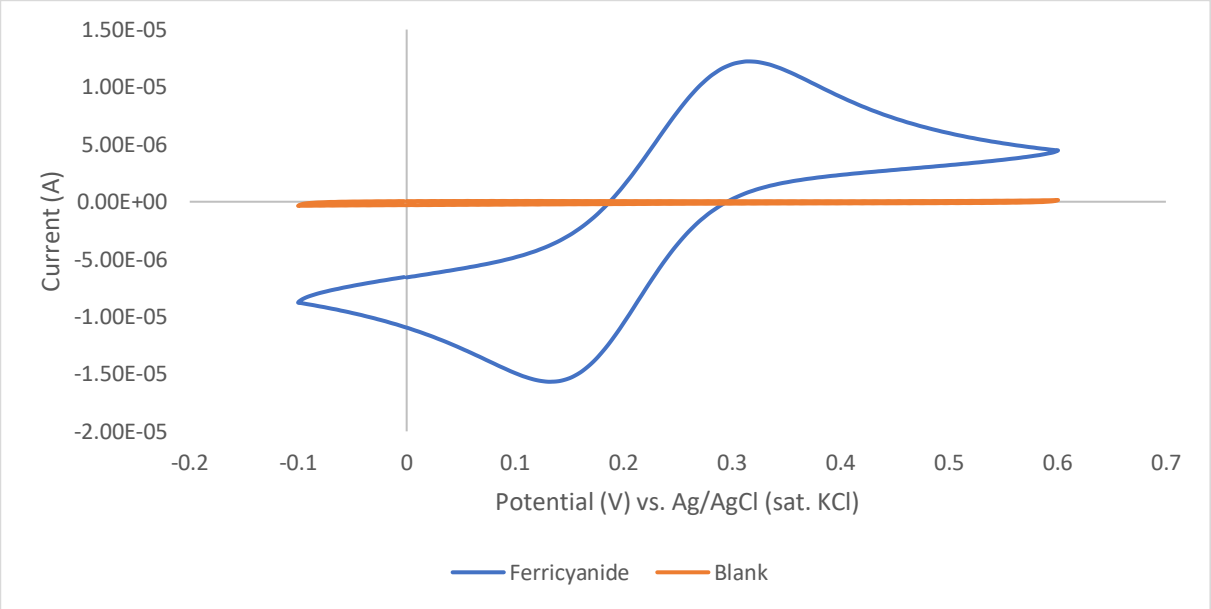

Figure 7: A representative voltammogram comparing a blank voltammogram with a ferricyanide voltammogram

In figure 7, a blank solution voltammogram is compared to a ferricyanide-containing solution for comparison.

The maximum and minimum peak currents were plotted vs √v for each fresh potassium ferricyanide solution. Linearity was found for each individual measurement, with all individual $R^2 > 0.99$.

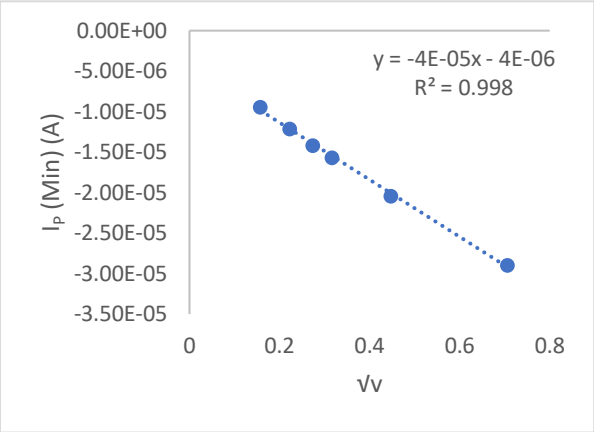

Figure 8: Reduction of ferricyanide

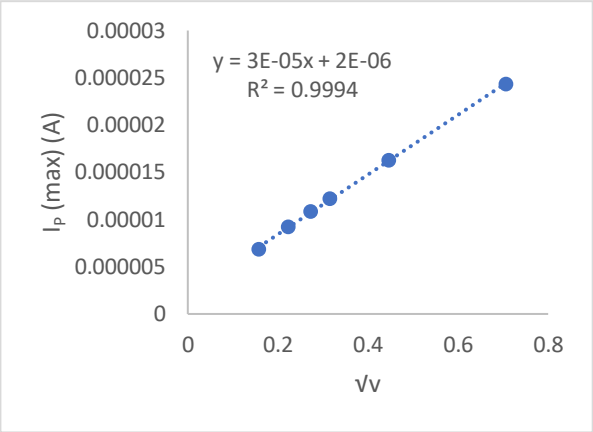

Figure 9: Oxidation of ferrocyanide

Figures 8 and 9 show the relationship between I_P and √v. R^2 is almost equal to 1, which indicates that a linear relationship between I_P and √v exists. As there is a linear relationship between I_P and √v and R^2 is close to 1, the system can be considered diffusion controlled. A diffusion-controlled system means that the system of electron transfer between the electrode and the species is only limited by the speed at which the species can diffuse to the electrode from the bulk solution (8).

Plots for a single set of measurements have been shown as examples in figures 6 to 9. For the rest of the cyclic voltammograms and *I_P vs √v relationship graphs* of the other two datasets for scan rate studies, see figures A1 through A6 in the appendix.

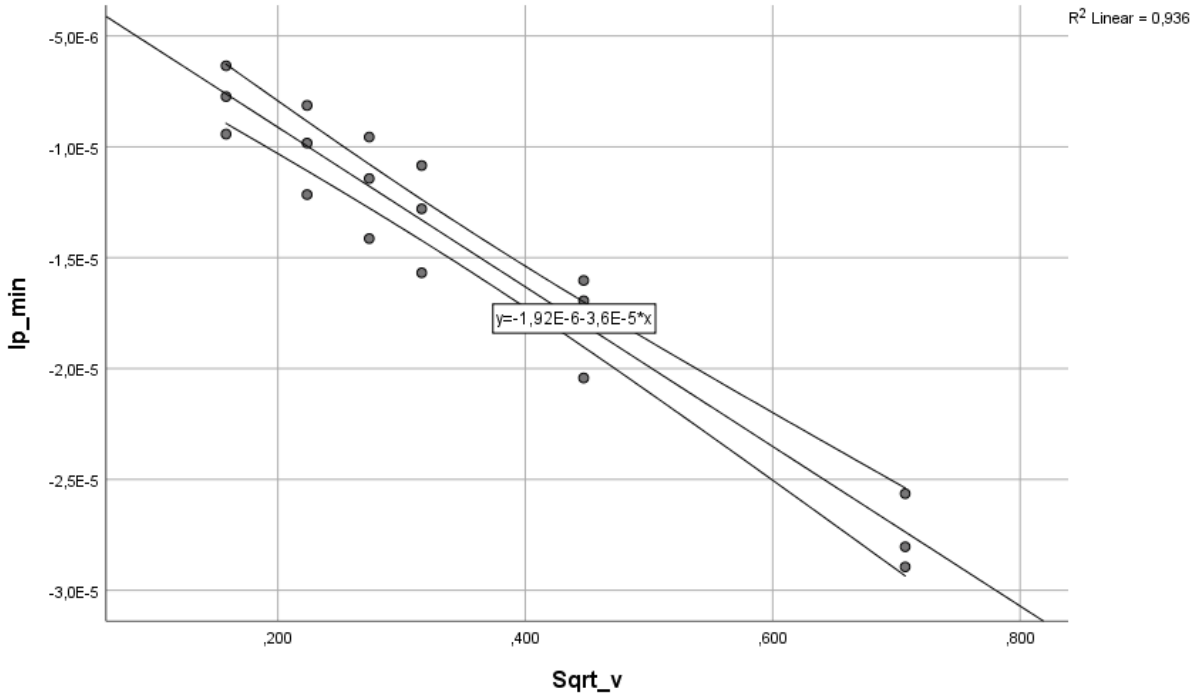

Figure 10: Scatter plot of the peak currents for the reduction of ferricyanide

The scatter plot includes the mean 95% confidence interval, and the regression line formula is Y = 1.92E-6 – 3.59E-5x with an R^2 value of 0.936.

The formula for Y shows that the intercept (B_0) = 1.92E-6 with p > 0.05 (associated with H_0: B_0 = 0), thus H_0 must not be rejected, and B_0 does not significantly deviate from 0, thus the line goes through the origin. Y shows slope (B_1) = -3.59E-5 with p < 0.05 (associated with H_0: B_1 = 0), thus H_0 should be rejected, and B_1 significantly deviates from 0 and there is regression. The slope can be used to determine the diffusion coefficient for the reduction of ferricyanide using the formula $D_R = B_1 / (k*n^{1.5}*A*C)$, which gives D_R = 1.72E-06 m^2/s. This value for D_R is similar in magnitude to the theoretical D_R, which was determined to be 6.67E-06 m^2/s (9)*. The difference between D_R values might be caused by different conditions or dissimilarities in the experimental setups, like the use of a platinum electrode* (9) *instead of a glassy carbon electrode, or deaeration of the solutions using presaturated nitrogen prior to use* (9).

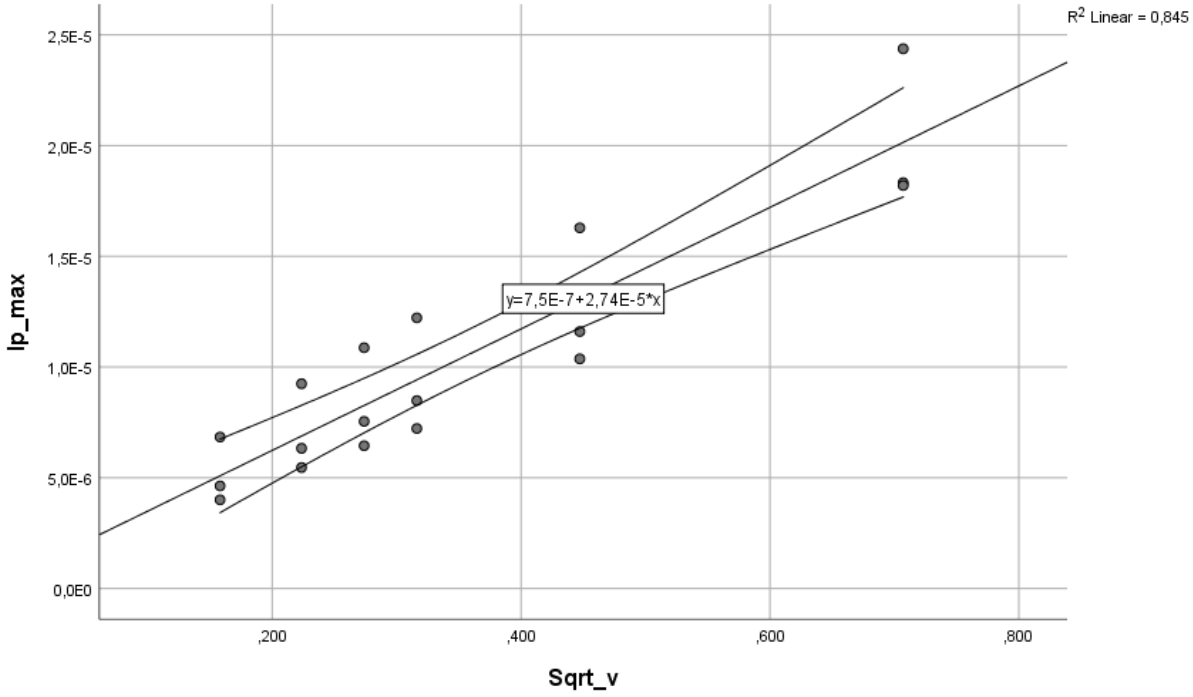

Figure 11: Scatter plot of the peak currents for the oxidation of ferrocyanide

The scatter plot includes the mean 95% confidence interval, , and the regression line formula is Y = 7.5E-7 + 2.74E-5x with an R^2 value of 0.845.

The formula for Y shows that the intercept (B_0) = 7.5E-7 with p > 0.05 (associated with H_0: B_0 = 0), thus H_0 must not be rejected, and B_0 does not significantly deviate from 0. Y shows slope (B_1) = 2.74E-5 with p < 0.05 (associated with H_0: B_1 = 0), thus H_0 should not be rejected, and B_1 significantly deviates from 0 and there is regression. The slope can be used to determine the diffusion coefficient for the oxidation of ferrocyanide using the formula $D_O = B_1 / (k*n^{1.5}*A*C)$, which gives D_O = 9.97E-07 m^2/s. This value for D_O differs in magnitude to the theoretical D_O, which was determined to be 7.26E-06 m^2/s (9). The determined diffusion coefficient values do not follow the same trend as the theoretical values. For the theoretical values, D_O is larger than D_R, but for out determined values, D_O is smaller than D_R.

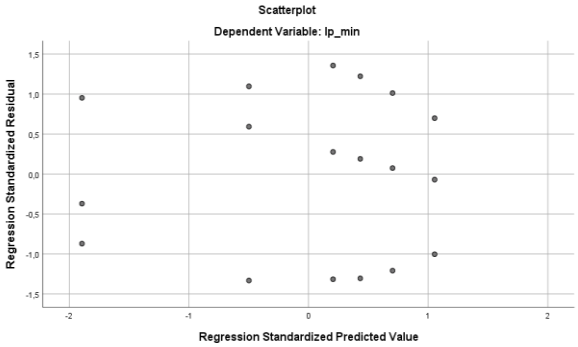

Figure 13: Residuals plot of the regression analysis for the reduction of ferricyanide

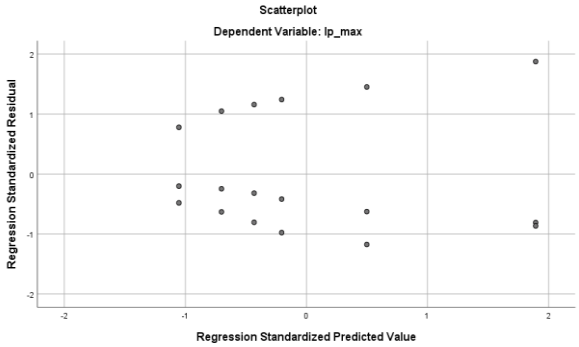

Figure 12: Residuals plot of the regression analysis for the reoxidation of ferrocyanide

The residuals plots show that data are not randomly distributed around the residual line. Figure 13 shows a clear pattern of increasing residual with increasing predicted values. Figure 12 shows more of a parabola-like pattern, with residuals increasing towards a predicted value of 0.

The data in the residuals plots show heteroscedasticity; the variance of the residuals is unequal over the experiment range and show a double horn-shaped pattern in figure 12, and a single horn-shaped pattern in figure 13. These horn shaped patterns indicate non-constant standard deviation of random errors. Usually, data is assumed to be of equal quality when used for estimations about a model. However, in case of non-constant standard deviation of random errors, the data is not actually of equal quality. This can be seen in figures 12 and 13 as the points are not randomly distributed through the plot, but show a pattern. Due to the presence of heteroscedasticity, the assumption of linear regression is unclear, but it does not prove whether there is linear regression or not. In the case of this experiment, the sample size is not big enough to make an accurate assumption based on the residuals plot, and more data points are necessary to determine whether the assumption of linear regression is correct or incorrect. (10)

4.2 Cyclic voltammetry experiments with hemin

Hemin is practically insoluble, but stable, in water (11). *This can be seen when looking at the structure of hemin: a big, non-polar molecule, long carbon chains and only a few atoms capable of forming H-bonds. Most metalloporphyrins have a pKa of around 4* (12)*, and pKa of carboxylic acids, of which hemin has two, are around 5* (12)*. A pH of 8 was used in all solutions used, as carboxylic acids are ionized at higher pH, which increases the solubility of hemin in water. Also, surfactant (SDS) was used, which forms micelles, further increasing the solubility in water. As mentioned, solely SDS was used as surfactant instead of in combination with TMAB. Although the micelles by these surfactants are comparable, some difference in uniformity are present* (13)*. The problems with water solubility of hemin could have all been circumvented by using an organic solvent, but in order to work as environmentally friendly as possible, the use of organic solvents is undesired.*

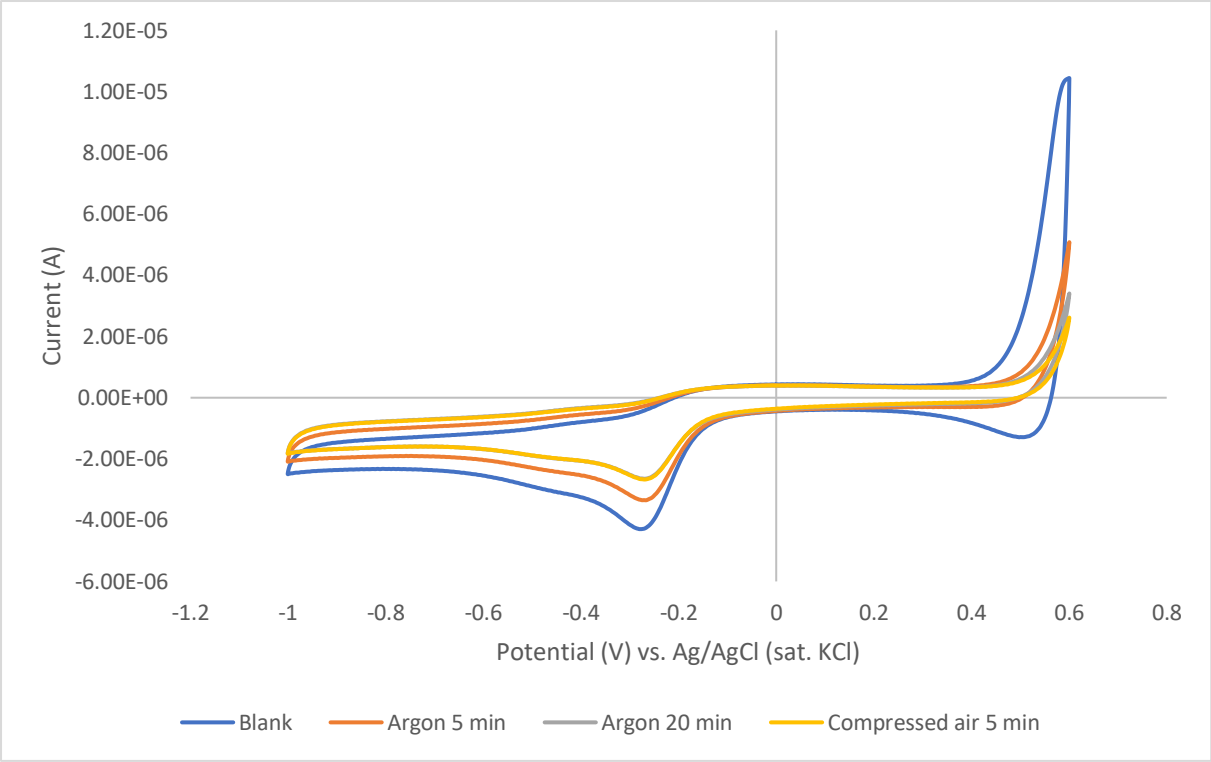

Figure 14: Showing the effect of sparging with argon on the oxygen reduction in the solution

The graph shows a decreasing I_P for the reductive current at around -0.25 V as time of sparging a blank solution with argon increases from 5 minutes to 20 minutes. No difference can be seen after aerating the solution for 5 minutes after it was sparged with argon for 20 minutes.

Figure 14 shows how the voltammogram of the blank buffer solution looks before adding any hemin, and compares the oxygen reduction peaks before and after sparging with argon and after aerating with compressed air to reintroduce oxygen into the solution, in the order: [1] before sparging, [2] argon 5 minutes, [3] argon 20 minutes, [4] compressed air 5 minutes. As argon is a heavy, inert gas, it is a suitable option to use in order to remove the oxygen in solution. As oxygen is reduced in water in the potential range used in this experiment (-1 V to 0,6 V), it can interfere with other peaks in the area, and thus argon sparging is performed to reduce the amount of oxygen in the solution. This can be observed in the figure by the decreasing reduction peak at approximately -0.3 V after sparging with argon, and we can assume that this peak belongs the oxygen reduction. However, the lack of difference after aerating and after the solution was sparged for 20 minutes with argon is unexpected. The hypothesis was that this peak will become greater in magnitude, but it remained almost exactly the same. The lack of change in I_P is probably due to the fact that argon is a heavy gas and is much harder to displace than air and might also be due to the fact that aerating was performed at way too low of a rate, which might have resulted in less oxygen being re-introduced into the solution.

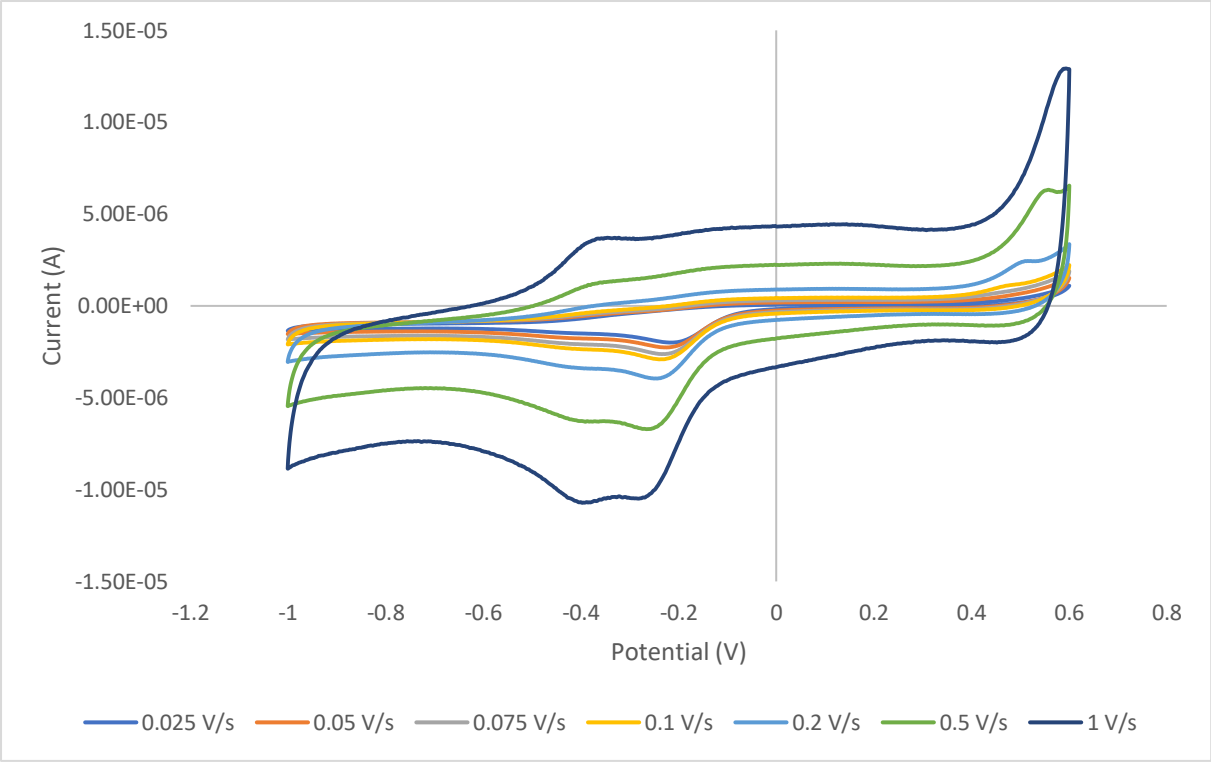

Figure 15: The first of two performed scan rate studies (H1) of the hemin solution, with scan rates ranging from 0.025 V/s to 1 V/s

A clear peak is observed at approximately -0.2 V to -0.3 V in the reductive scans, shifting to more negative potentials with increasing scan rates. At higher scan rates (0.2 V/s and higher), a second reduction peak becomes visible at approximately -0.4 V, partly covered by the first peak. At higher scan rates, the oxidative peak becomes more visible at -0.4 V. A small oxidation peak at approximately 0.5 V is visible at 0.2 V/s and 0.5 V/s, but is not present at any other scan rate.

In presence of hemin, a new peak arises approximately between -0.3 and -0.4 V, thus it is suggested and assumed that this peak belongs to the reduction of hemin (or a hemin-related species). As increasing scan rate leads to increasing peaks due to the relation between I_P and √v, peaks that might be less visible at lower scan rates become more visible at higher scan rates. This relationship between I_P and √v causes the reduction peak for hemin at -0.4 V to become more noticeable at higher scan rates. ΔE_p seems to change randomly, and $E_{1/2}$ seems to become slightly less negative. This shift in $E_{1/2}$ suggests an earlier onset of reduction due to a structural change. The solution was sparged with argon for 20 minutes before the experiment. Sparging with argon for 20 minutes was done to minimize the oxygen reduction peak in the voltammogram in order to increase the resolution of any hemin-related peaks, as the oxygen reduction peak may engulf any other peaks in the area if it is not removed from the solution. But as the oxygen reduction peak is still visible, it means that 20 minutes of sparging with argon might not be enough to get rid of all oxygen.

Table 2: ΔEP and E1/2 of the voltammograms shown in figure 15

Scan rate (V/s)	*0.025*	*0.05*	*0.075*	*0.1*	*0.2*	*0.5*	*1*
$E_{1/2}$ (V)	*-0.38452*	*-0.37354*	*-0.36987*	*-0.37598*	*-0.37598*	*-0.37109*	*-0.37231*
ΔE_p (mV)	*31.74*	*9.77*	*17.09*	*24.41*	*9.76*	*39.06*	*51.27*

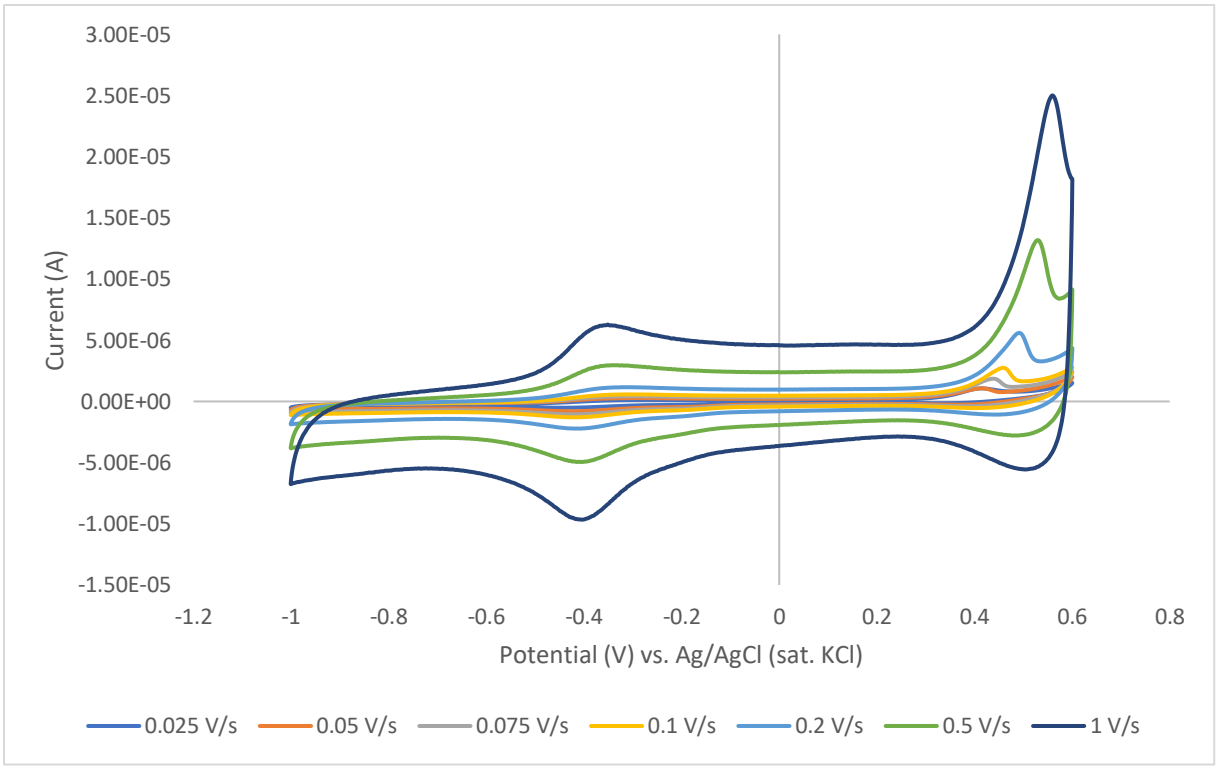

Figure 16: The second of two performed scan rate studies (H2) of the hemin solution, with scan rates ranging from 0.025 V/s to 1 V/s

A peak can be clearly seen at approximately -0.4 V, and the wave shows a return peak at approximately -0.35 V. This set of voltammograms contains an additional, clear peak at around 0.5 V.

Here, the solution was sparged with argon at a much higher rate (observed by increasing bubbling) for 20 minutes before the experiment. Sparging with argon at a high rate led to the complete disappearance of the oxygen reduction peak at around -0.3 V, making the peak that is observed in the presence of hemin at -0.4 V much clearer. E_P for the reduction and oxidation move towards each other with increasing scan rate, which can be seen in table 1 by the decreasing ΔE_P values with increasing scan rates. This change in E_P indicates electrochemical irreversibility. Electrochemical irreversibility can be caused by [1] a chemical step after the initial reduction of hemin, inhibiting the re-oxidation, or [2] due to adsorption to the electrode surface. As a return oxidation peak can be observed in figure 11, it is unlikely that the electrochemical irreversibility is caused by a chemical step. $E_{1/2}$ becomes more negative with increasing scan rate. This shift in $E_{1/2}$ suggests a later onset of reduction due to a structural change. The additional peak at 0.5 V was only clearly observed in this set of CV runs. This peak also appears in figure 13, for the high rate of argon sparging. The appearance of this peak indicates that this peak might only be visible when the amount of oxygen in solution is practically zero. However, we cannot say much more about it without more evidence as to what it might be.

Table 3: ΔEP and E1/2 of the voltammograms shown in figure 16

Scan rate	*0.025 V/s*	*0.05 V/s*	*0.075 V/s*	*0.1 V/s*	*0.2 V/s*	*0.5 V/s*	*1 V/s*
$E_{1/2}$ (V)	*-0.35522*	*-0.35645*	*-0.35889*	*-0.36133*	*-0.35889*	*-0.37476*	*-0.37720*
ΔE_p (mV)	*168.46*	*131.84*	*131.84*	*112.30*	*107.42*	*61.04*	*51.27*

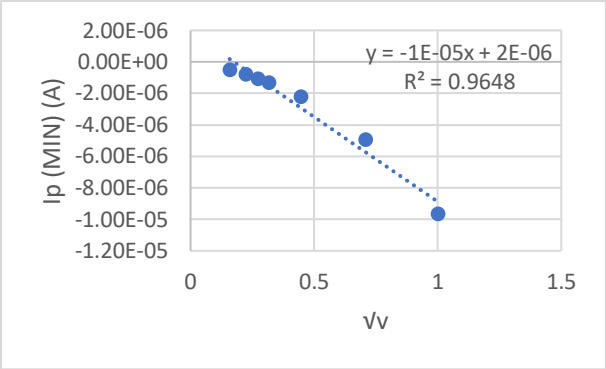

Figure 17: Reduction of hemin

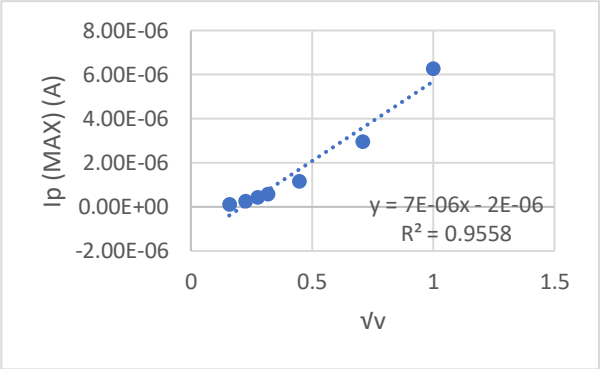

Figure 18: Reoxidation of hemin

Figures 17 and 18 show the relationship between I_P and √v for the scan rate study of hemin (H2, figure 16). R^2 values are 0.965 for the reduction, and 0.956 for the oxidation.

There seems to be a linear relationship between I_P and √v, *but there is a slight curve in the data points. The curve in the data indicates a less strong linear correlation, as can be seen by the* R^2, *which is smaller than the* R^2 *seen for ferricyanide. This non-linearity could mean that this system is not a diffusion-controlled system, which was seen to be the case for ferricyanide, indicating that the observed current is not just related to the diffusion of the electroactive species to the electrode, but allows the possibility of other phenomena like adsorption of the species onto the electrode to also contribute to the observed potential, leading to the less strong linear correlation* I_P and √v.

Plots for a single set of measurements have been shown as examples in figures 17 and 18. For the plots for H1 (figure 15), see figures B1 and B2 in the appendix.

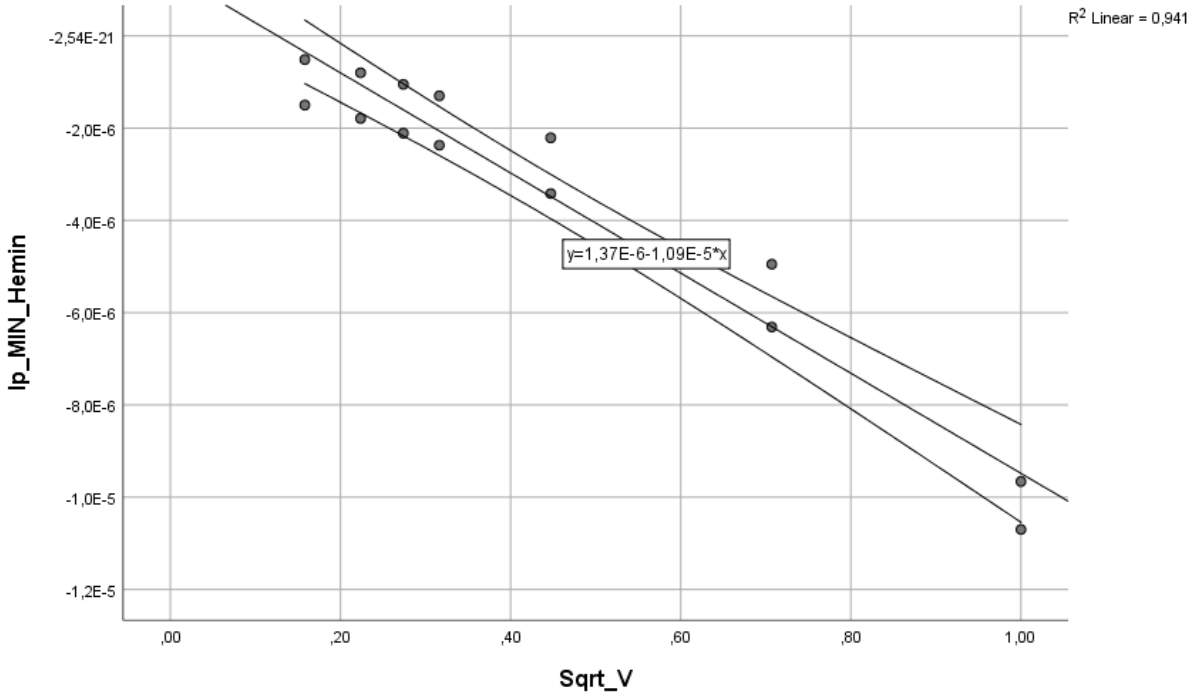

Figure 19: Scatter plot of the peak currents for the reduction of hemin

The scatter plot includes the mean 95% confidence interval, and the regression line formula is Y = 1.37E-6 – 1.09E-5X, with an R^2 value of 0.941.

The formula for Y shows that the intercept (B_0) = 1.37E-6 *with* $p < 0.05$ *(associated with* H_0: $B_0 = 0$*), thus* H_0 *must be rejected, and* H_A *should be accepted, and* B_0 *significantly deviates from 0. Y shows slope* (B_1)

= 1.09E-5 with p < 0.05 (associated with H_0: B_1 = 0), thus H_0 should be rejected, and H_A should be accepted, so B_1 significantly deviates from 0 and there is regression.

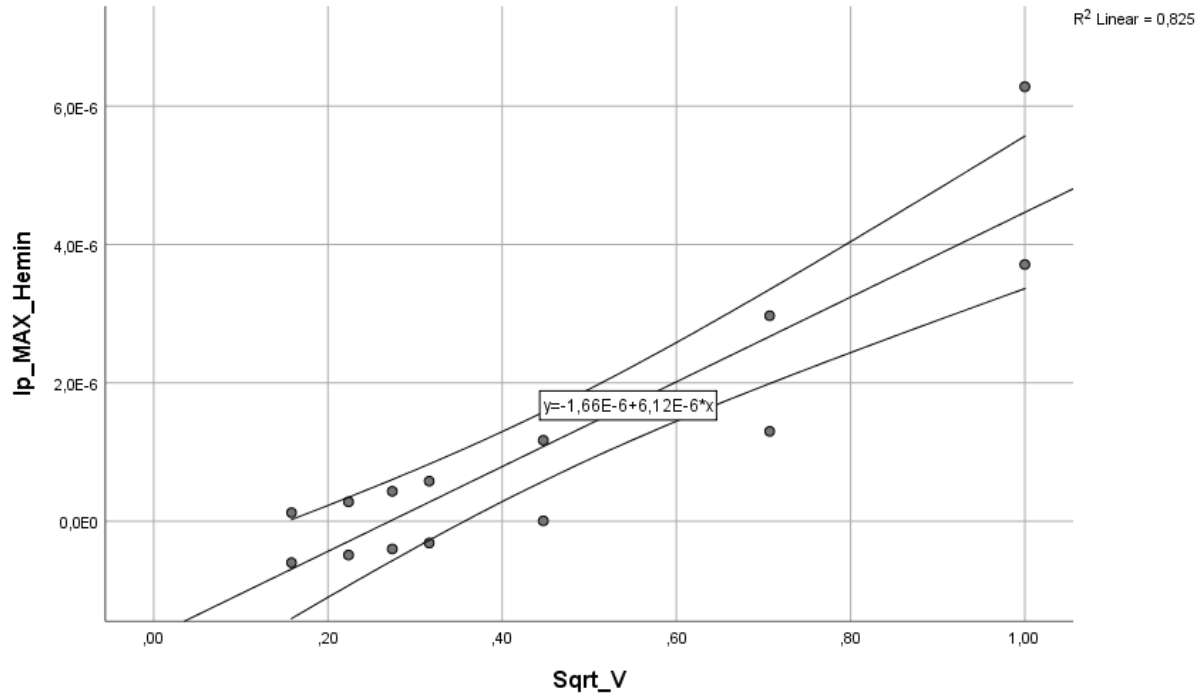

Figure 20: Scatter plot of the peak currents for the reoxidation of hemin

The scatter plot includes the mean 95% confidence interval, and the regression line formula is Y = -1.66E-6 + 6.12E-6X, with an R^2 value of 0.825.

The formula for Y shows that the intercept (B_0) = -1.66E-6 with p < 0.05 (associated with H_0: B_0 = 0), thus H_0 must be rejected, and H_A should be accepted, and B_0 significantly deviates from 0. Y shows slope (B_1) = 0.03 with p < 0.05 (associated with H_0: B_1 = 0), thus H_0 should be rejected, and H_A should be accepted, so B_1 significantly deviate from 0 and there is regression.

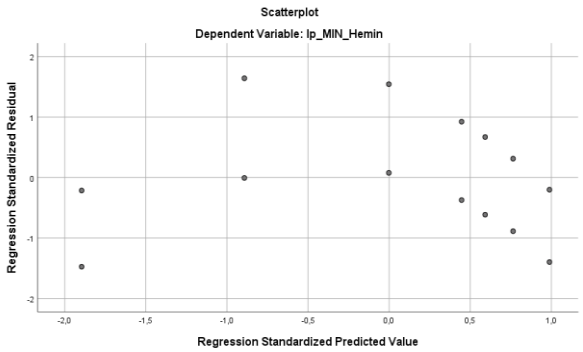

Figure 21: Residuals plot of the regression analysis for the reduction of hemin

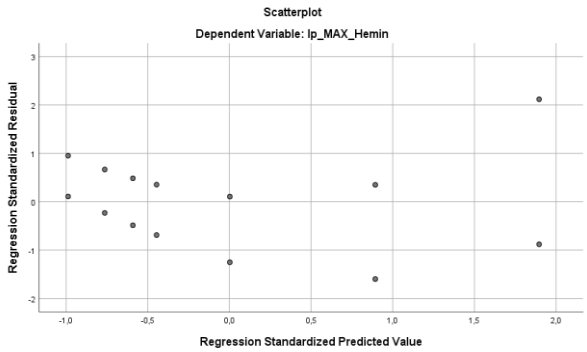

Figure 22: Residuals plot of the regression analysis for the reoxidation of hemin

The residuals plots show that data are not randomly distributed around the residual line.

The data in the plots in figures 21 and 22, like figures 12 and 13, show a pattern and are not randomly distributed and show heteroscedasticity, thus the assumption of linear regression is unclear.

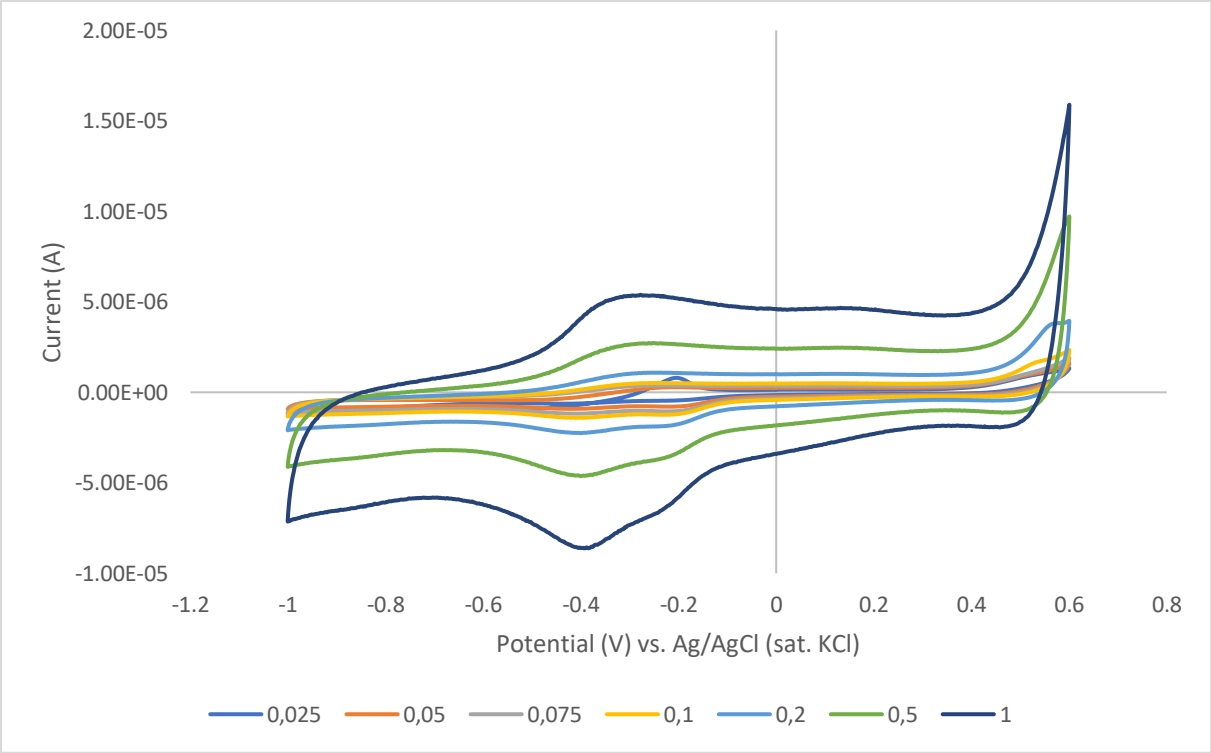

Figure 23: A scan rate study of the hemin/pyridine solution

A small peak is seen at around -0.25 V. A larger peak can be seen at -0.4 V. All peaks at -0.4 V are slightly smaller in these hemin/pyridine voltammograms compared to the hemin voltammograms, except for the oxidation peak at scan rate 0.025 V/s.

The presence of pyridine seems to have an effect on $E_{1/2}$. Figure 23 and table 4 shows $E_{1/2}$ moving to more negative potentials with increasing scan rate, which follows the same trend as the data in figure 16, and in the opposite trend as the data in figure 15, where $E_{1/2}$ moves towards more positive potentials. In figure 23, a smaller reduction I_P is observed compared to figure 15. When pyridine binds to hemin, the hemin will become penta-coordinated. This 5-coordinated hemin, upon reduction, becomes a high-spin molecule which is a good oxygen binder. Due to the much smaller oxygen reduction I_P in figure 23, it is suggested that pyridine has indeed bound to hemin, and it has become a high-spin molecule which has bound oxygen from solution. A comparison between table 2 and 4, representing the data in figures 15 and 23 respectively shows an average $E_{1/2}$ shift of 0.049 V to more positive potentials when pyridine is present. This shift in $E_{1/2}$ suggests an earlier onset of reduction due to a structural change. This is also seen in the study of Compton. D, where whenever hemin was dissolved in pyridine in order to form hemin/pyridine complexes, $E_{1/2}$ would decrease compared to situations where hemin was not complexed with pyridine (14).

Table 4: ΔEP and E1/2 of the voltammograms shown in figure 23

Scan rate	0.025 V/s	0.05 V/s	0.075 V/s	0.1 V/s	0.2 V/s	0.5 V/s	1 V/s
$E_{1/2}$ (V)	*-0.31983*	*-0.31738*	*-0.32715*	*-0.32227*	*-0.32593*	*-0.33203*	*-0.33569*
ΔE_p (mV)	*234.38*	*209.96*	*170.90*	*175.78*	*148.93*	*117.19*	*114.75*

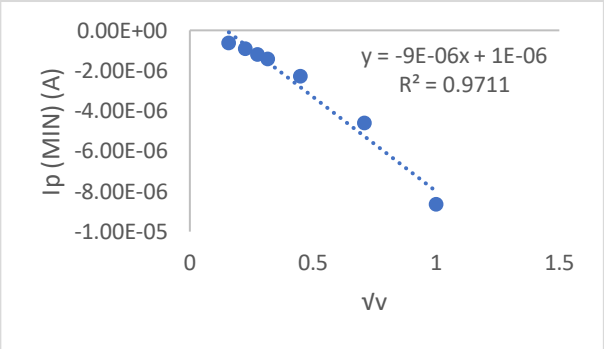

Figure 24: Reduction of hemin

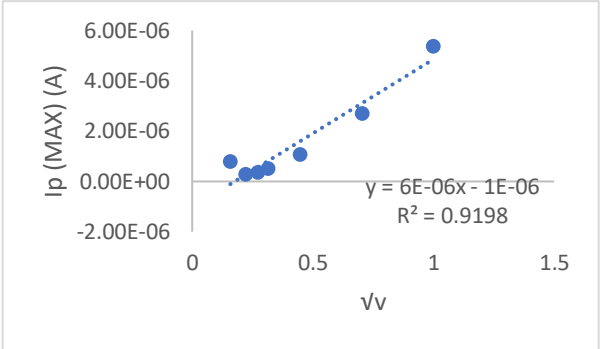

Figure 25: Reoxidation of hemin

Figures 24 and 25 show the relationship between I_P and √v for the scan rate study of hemin (H2, figure 16). R^2 values are 0.971 for the reduction, and 0.920 for the oxidation. There seems to be a linear relationship between the two, but there is a slight curve in the data points. This indicates that there is some adsorption to the electrode, as otherwise R^2 would be closer to 1 and there would not be a curve.

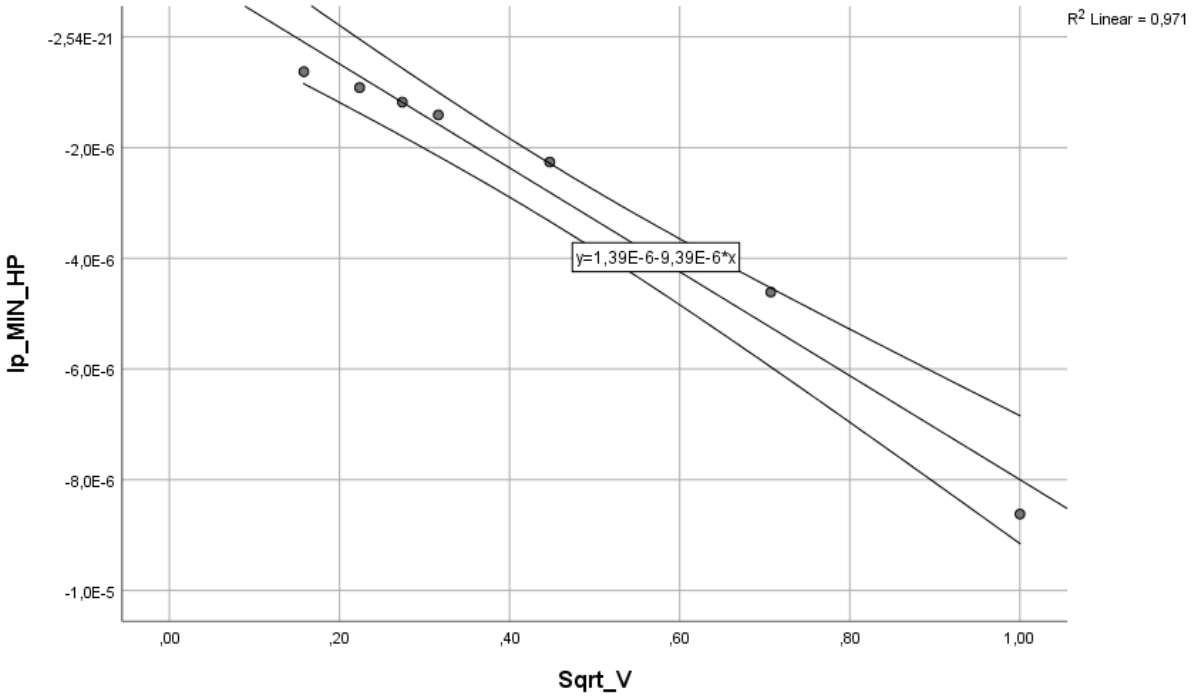

Figure 26: Scatter plot of the peak currents for the reduction of hemin

The scatter plot includes the mean 95% confidence interval, and the regression line formula is Y = 1.39E-6 – 9.39E-6X, with an R^2 value of 0.971.

The formula for Y shows that the intercept (B_0) = 1.39E-6 with $p < 0.05$ (associated with H_0: $B_0 = 0$), thus H_0 must be rejected, and H_A should be accepted, and B_0 significantly deviates from 0, meaning that the line does not go through the origin. Y shows slope (B_1) = -9.39E-6 with $p < 0.05$ (associated with H_0: $B_1 = 0$), thus H_0 should be rejected, and H_A should be accepted, so B_1 significantly deviates from 0 and there is regression.

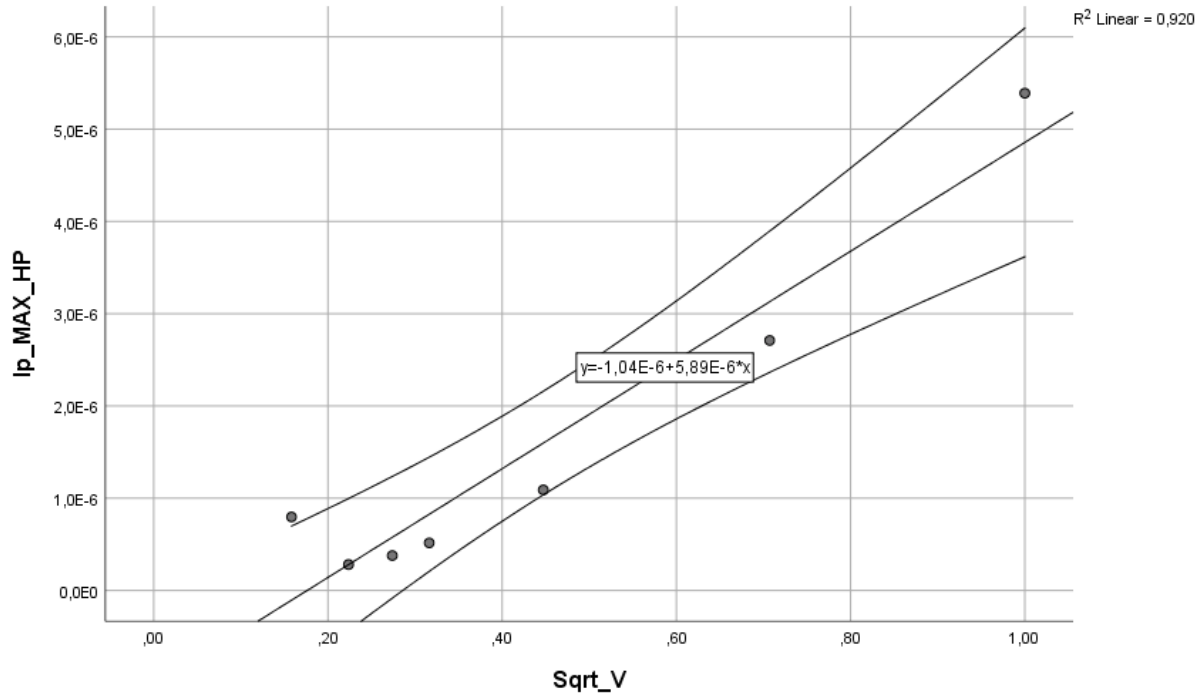

Figure 27: Scatter plot of the peak currents for the reduction of hemin

The scatter plot includes the mean 95% confidence interval, and the regression line formula is Y = -1.04E-6 + 5.89E-6X, with an R^2 value of 0.920.

The formula for Y shows that the intercept (B_0) = -1.0E-6 with p > 0.05 (associated with H_0: B_0 = 0), thus H_0 must not be rejected, and B_0 does not significantly deviate from 0, meaning that the line goes through the origin. Y shows slope (B_1) = 5.89E-6 with p < 0.05 (associated with H_0: B_1 = 0), thus H_0 should be rejected, and H_A should be accepted, so B_1 significantly deviates from 0 and there is regression.

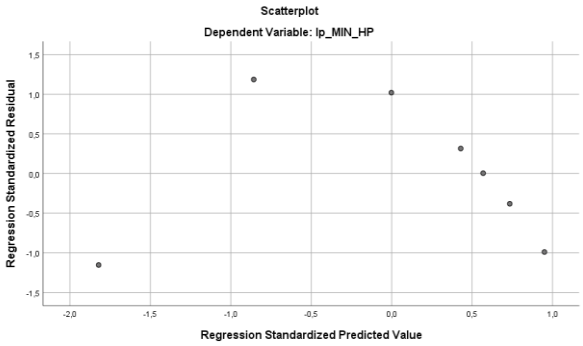

Figure 28: Residuals plot of the regression analysis for the reduction of hemin in presence of pyridine

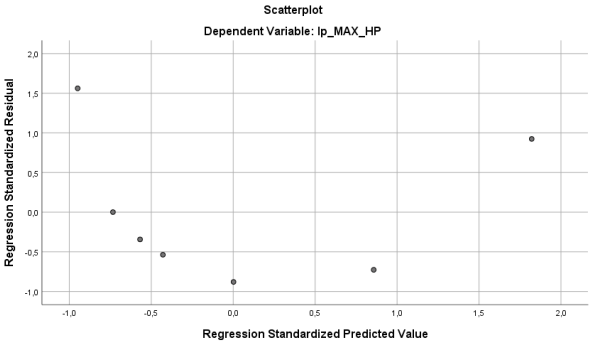

Figure 29: Residuals plot of the regression analysis for the reoxidation of hemin in presence of pyridine

The residuals plots show that data are not randomly distributed around the residual line, but show a parabola-like pattern.

The data in the plots in figures 28 and 29, like figures 12, 13, 21 and 22, show a pattern and are not randomly distributed and show heteroscedasticity, thus the assumption of linear regression is unclear.

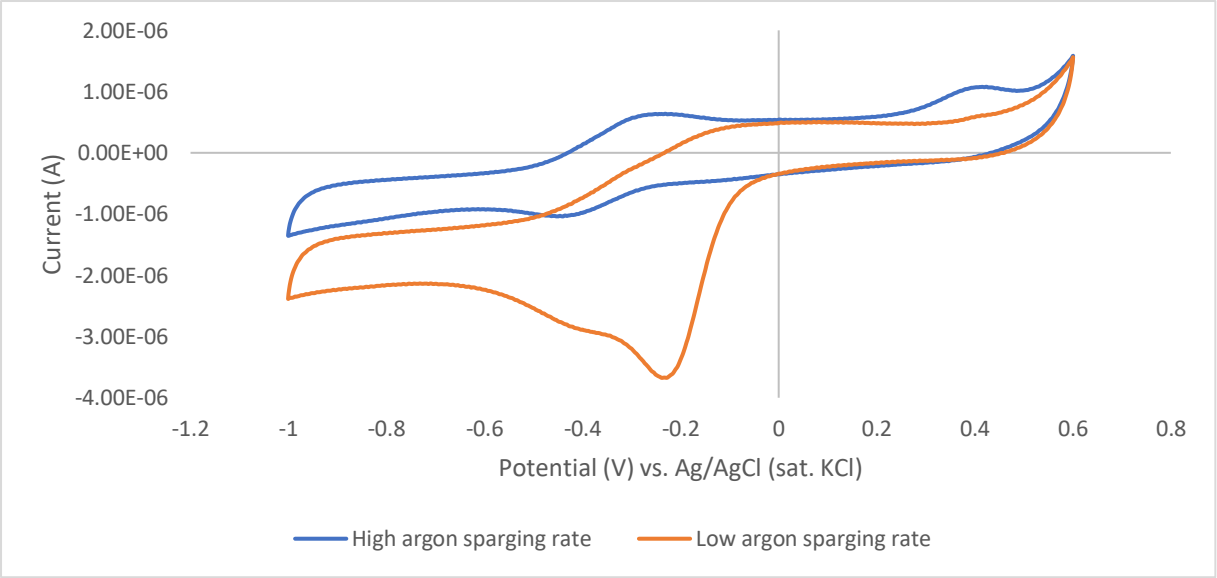

Figure 30: A comparison between argon sparging rate of two hemin solutions with equal concentration

A higher rate of argon sparging has much smaller peaks for oxygen and hemin.

*To see whether sparging was done correctly and had sufficient effect on the amount of oxygen in solution during the experiments, a comparison was made between the method of argon sparging used during the experiments (low rate) and a higher rate of sparging. One solution with a hemin concentration of 8,9868*10^{-3} M was used in both tests. High argon sparging rate shows to remove much more oxygen from the solution as expected, suggesting that the peak at around -0.2 V indeed belongs to oxygen reduction. Due to the absence of this oxygen peak, the hemin peak is not covered by the relatively larger oxygen reduction peak, making the hemin peak at -0.4 V clearer and more visible.*

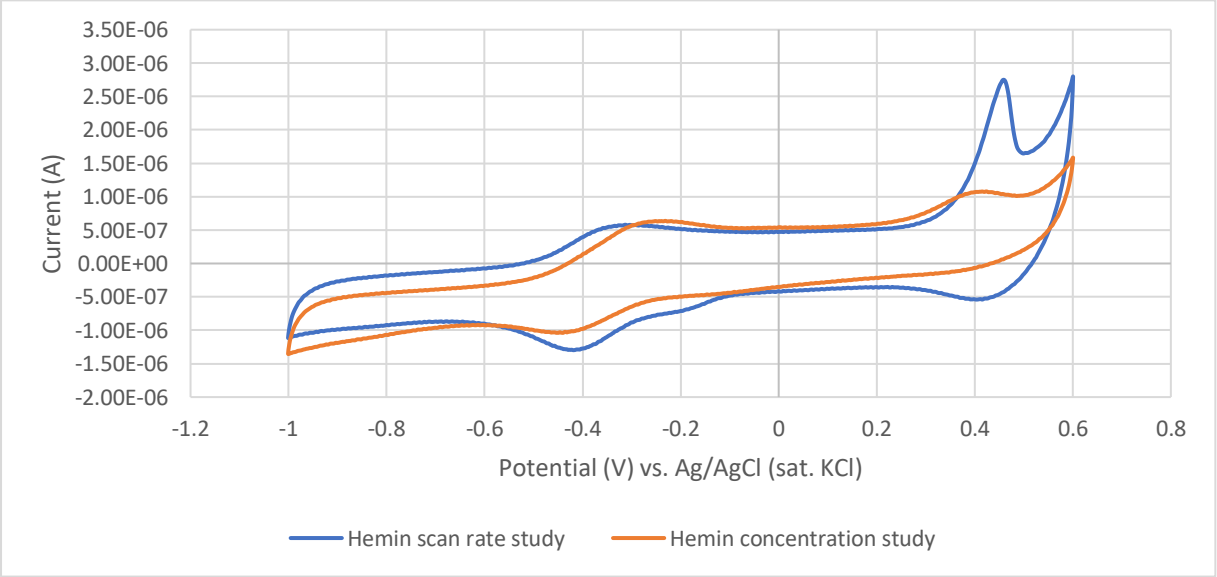

Figure 31: A comparison between two 9 mM hemin solutions, both sparged at a high rate with argon for 20 minutes

The voltammograms look similar, but at higher potential, some larger peaks can be seen in the scan rate study voltammogram.

Overall, the CVs are quite similar, but one difference exists. The scan rate study CV is the one at 0.1 V/s, similar to the concentration study. However, the scan rate study CV for 0.1 V/s was performed after

first performing scan rates of 0.025, 0.050, and 0.075, which means there was a time period between sparging and doing the scan rate test at 0.1 V/s scan rate. This time period was 20 minutes, and the possibility exists that during this time period, oxygen was reintroduced into the system, indicated by the small peak at approximately -0.2 V as shown in figure 14 for the hemin scan rate study. This time period was not present for the concentration study, as this was performed immediately after sparging with argon for 20 minutes, which can be a cause for the differences between the CVs.

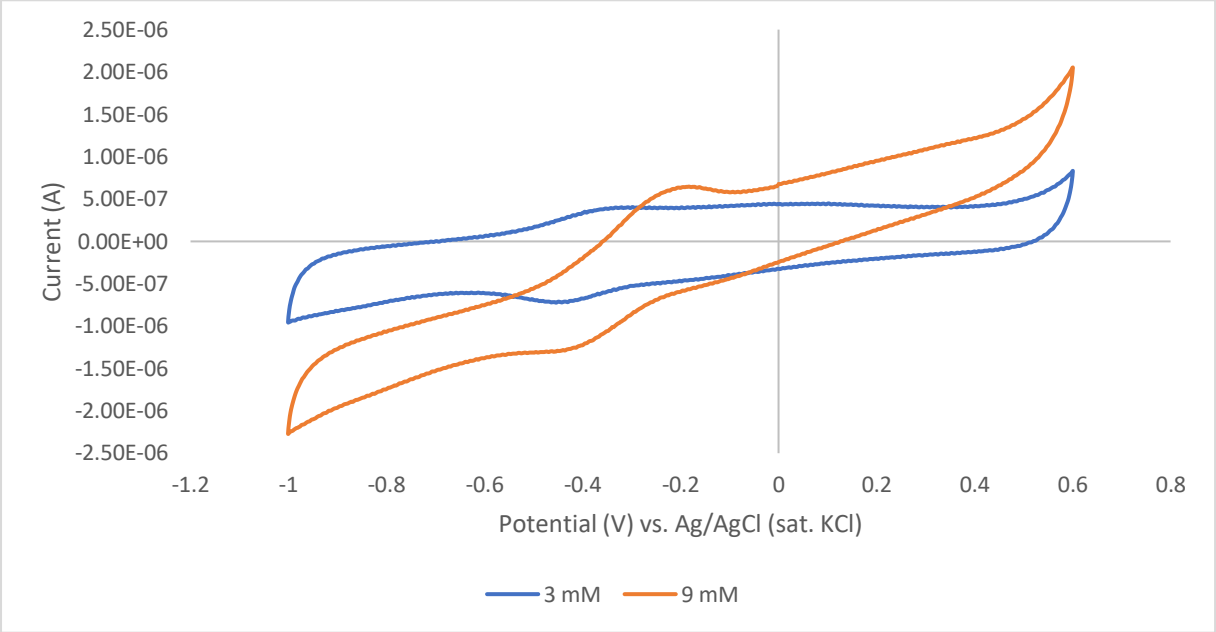

Figure 32: A comparison between 3 mM and 9mM hemin solution sparged at a high rate with argon

The oxygen peak at -0.4 V seems to have disappeared completely, leaving only the hemin peak. Also, the hemin peak is larger at higher hemin concentrations.

As the oxygen peak is completely absent, the hemin peak can be clearly observed. The comparison between hemin concentrations shows that the peak at approximately -0.4 V becomes larger when the hemin concentration increases, indicated by the greater I_P at approximately -0.4 V. The increase in I_P in presence of a higher hemin concentration suggests that the peak at -0.4 V belongs to hemin.

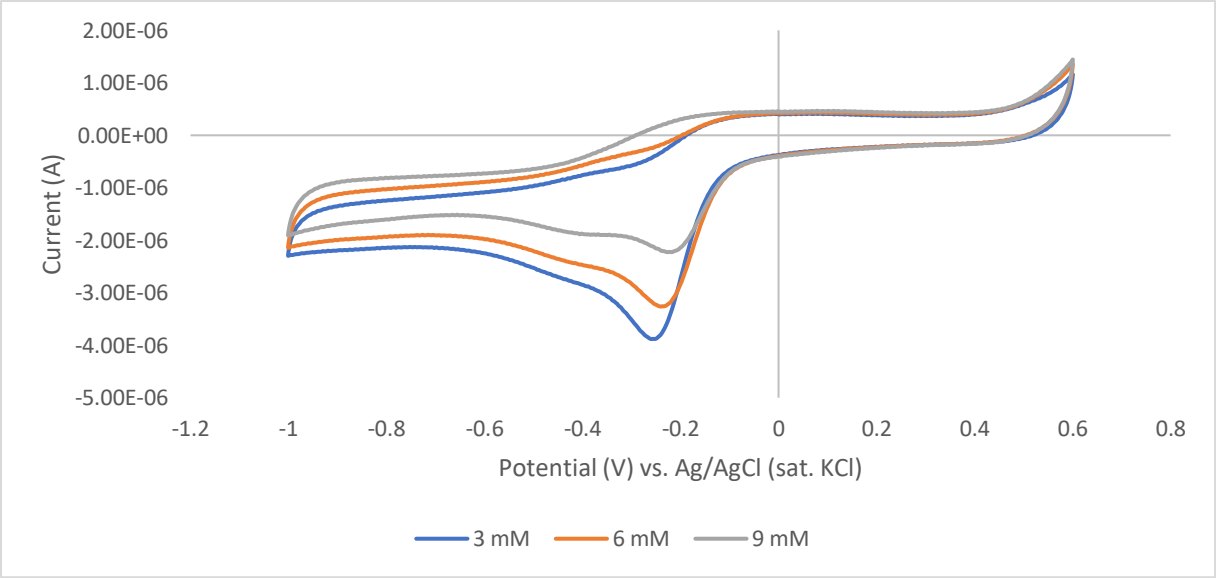

Figure 33: A concentration study of the hemin/pyridine solution

Here, with increasing hemin/pyridine concentrations, a clear decrease in reduction peaks, and an increase in oxidation peaks is observed.

Hemin is a 5-ligand molecule, surrounded by four pyrroles and a chloride ion. By adding pyridine, it will bind to hemin in the axial position (15)*, becoming a 6-coordinated molecule. When this hemin is reduced in the 5- or 6-coordinated form to* Fe^{2+}*, it becomes a high-spin heme molecule* (16)*. This high-spin* Fe^{2+} *is a strong oxygen binder* (17) *and in presence of oxygen will thus be oxidized by oxygen, forming* $Fe^{3+}O_2$*. This can be seen in the catalytic cycle of heme (figure 1): when* Fe^{3+} *is reduced by an electrode into* Fe^{2+} *in presence of oxygen, this* Fe^{2+} *will then bind to oxygen, taking priority over the reoxidation of* Fe^{2+} *into* Fe^{3+}*. When the hemin concentration increases, more oxygen will bind to* Fe^{2+}*, thus the oxygen reduction peak observed in figure 33 will become smaller. The increasing oxidation peak can be due to different possible reactions: [1] After oxygen binds to* Fe^{2+} *in step 3 of the catalytic cycle, the electrode can reduce this oxygen-bound* Fe^{3+} *into* Fe^{2+}*-*O_2*, and then reoxidate it to* Fe^{3+}*-*O_2*, [2] after oxygen has been bound in step 3 of the catalytic cycle, the electrode can reduce the iron-bound* O_2 *into* Fe^{3+}*-*O_2^- *as seen in step 4, and then reoxidate it into* Fe^{3+}*-*O_2*. These oxidations by the electrode will be seen in the return oxidation peak, which causes this peak to become larger with higher concentrations of hemin. On the other hand, an increase in hemin concentration will cause more oxygen to bind to* Fe^{3+}*, which will cause the oxygen reduction peak to become smaller, as seen in figure 33.*

4.3 Cyclic voltammetry experiments with hemin and substrates

Two substrates, fenbendazole and ASA, were assessed on reactivity in presence of hemin and pyridine (1:1 ratio, 0.5 mM). The substrates were added to solution in concentrations of 10 or 20 mM.

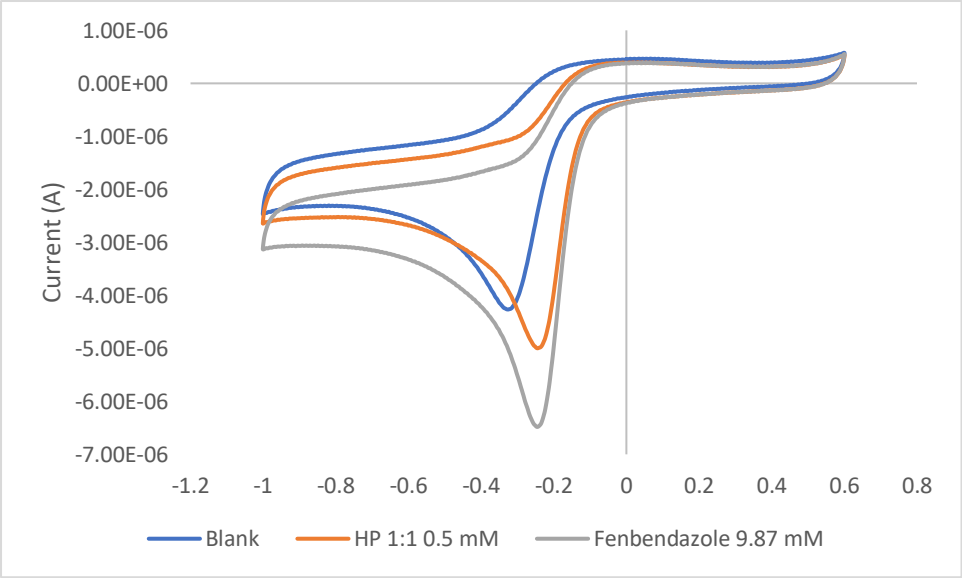

Figure 34: A voltammogram containing Fenbendazole, compared to a blank solution and a hemin/pyridine solution

Fenbendazole causes the peak at approximately -0.25 V to become larger.

Adding hemin/pyridine complex or fenbendazole causes the peak at -0.25 V to become larger. When hemin is added to the solution, it follows the catalytic cycle, which involves multiple reduction steps: [1] reduction of Fe^{3+} to Fe^{2+}, [2] reduction of $Fe^{3+}O_2$ to $Fe^{3+}O_2^-$, along with the direct reduction of oxygen which also happens in absence of hemin. The increase in reduction peak could be caused by these extra reduction steps. When we then add fenbendazole to the solution, a further increase of this peak is observed: the catalytic peak. This can be explained by the fact that fenbendazole is oxidized by the oxo-iron(IV) porphyrin, causing the appearance of a catalytic peak, as more current is going into the solution to perform the reducing steps in the catalytic cycle, but the reoxidation steps are being performed by the catalyst, and not by the electrodes, thus causing an increasing reduction peak along with a decreasing oxidation peak.

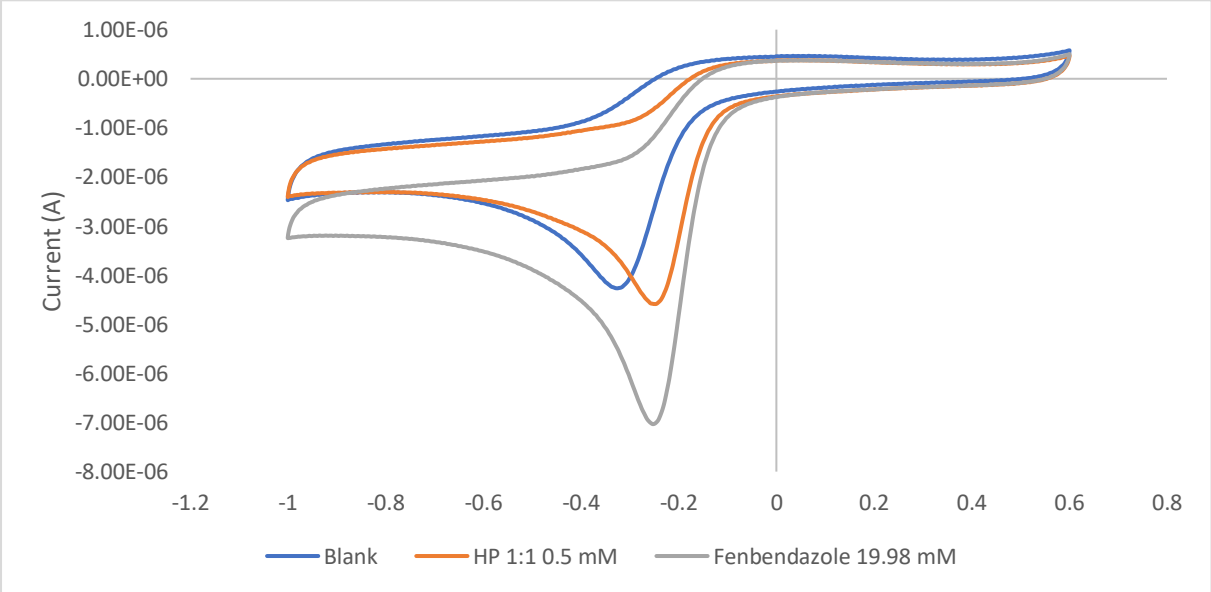

Figure 35: A voltammogram where the concentration of fenbendazole has been doubled

The peak at -0.25 V seems to be remarkably similar compared to when there is only half the concentration of fenbendazole, but seem to increase compared to the hemin/pyridine baseline.

As the peak at -0.25 V does not change with increasing fenbendazole concentration, it might indicate that the amount of oxygen in solution is the rate limiting step. If there is not enough oxygen present at the electrode for the reaction to proceed according to the catalytic cycle, increasing the substrate concentration would not cause an increase in the catalytic peak.

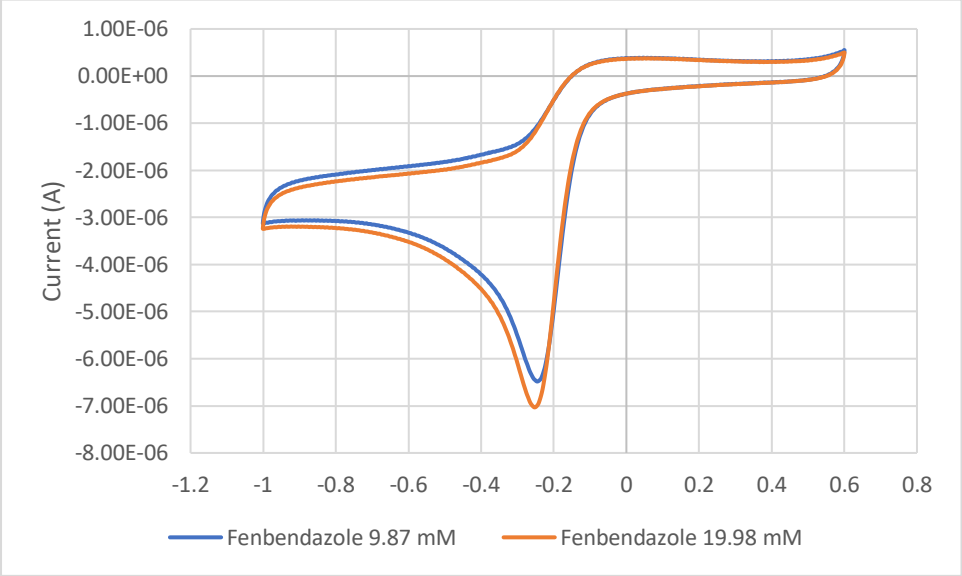

Figure 36: A comparison between the lower and higher concentrations of fenbendazole

There is only a slight increase in I_P when doubling the substrate concentration.

When comparing only the peaks when fenbendazole has been added, we only see a slight difference. However, when comparing the substrate peaks to their corresponding HP peaks, a slight increase in effect is seen in the peak belonging to the higher fenbendazole concentration, as the difference between the HP peak and substrate peak is larger. This can be seen when comparing figures 34 and 35.

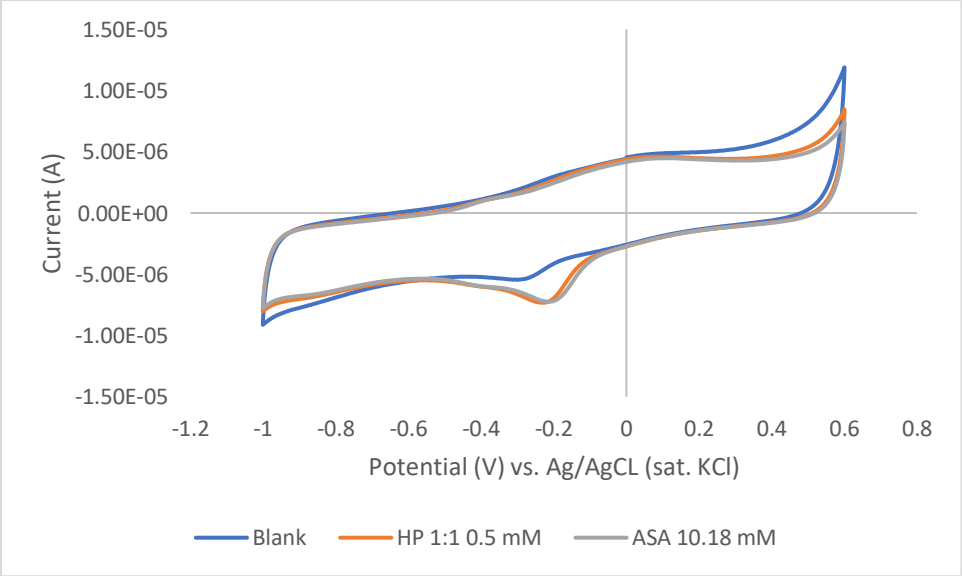

Figure 37: A voltammogram containing ASA, compared to a blank solution and a hemin/pyridine solution

No changes can be observed in the voltammogram after adding ASA.

As there is no change after adding ASA, we can assume that ASA is not reactive and is thus not metabolized by hemin.

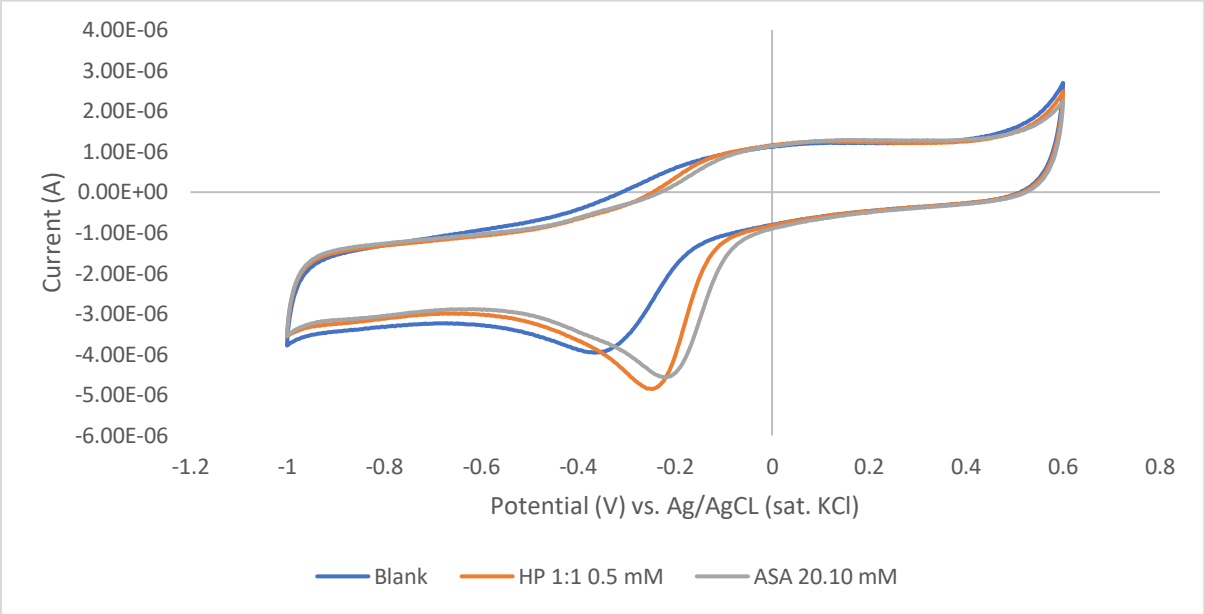

Figure 38: A voltammogram where the concentration of ASA has been doubled

Here, there seems to be a small difference causes by adding ASA, indicated by the slight shift in reduction E_P. A slight increase in oxidation E_p can also be observed.

A shift in E_P caused by ASA can indicate that ASA is metabolized, which happens at a slightly different potential. This earlier onset can cause the peak to shift slightly.

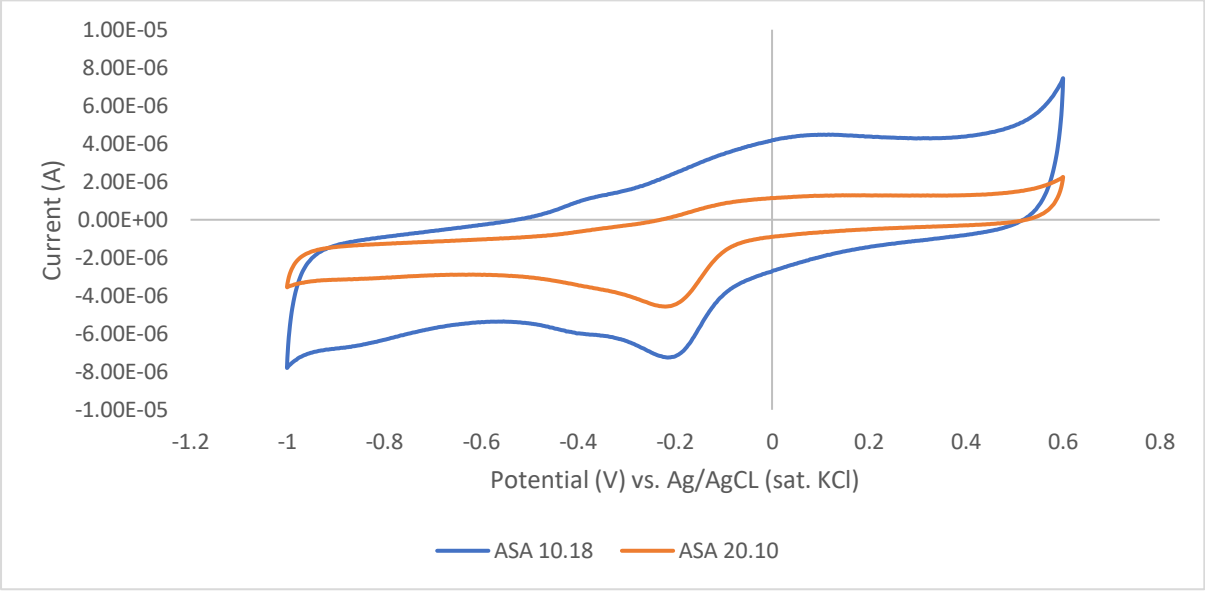

Figure 39: A comparison between the lower and higher concentrations of ASA

The solution with the higher ASA concentration shows a smaller reduction peak at -0.25 V.

The difference seen between the two lines in figure 39 are solely caused by the difference in baseline of the solutions (blank solution, hemin/pyridine complex solution), as when the ASA voltammograms are

compared with their respective solution voltammograms, the ASA lines overlap with the hemin/pyridine complex voltammograms.

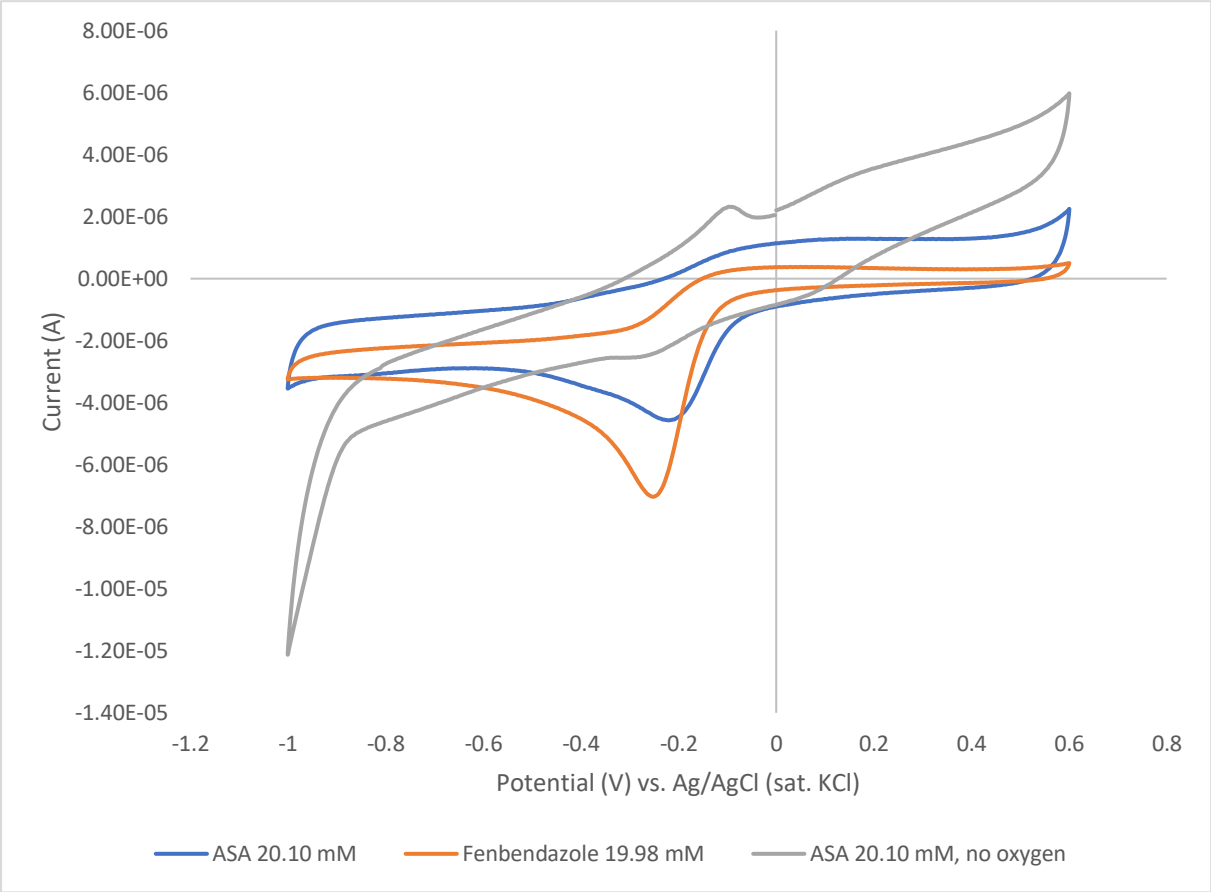

Figure 40: A comparison between the highest concentrations of substrate with the situation where oxygen is not present in solution

When there is no oxygen present, the substrate peak seems to be irreversible.

When there is no oxygen present in solution, step 3 in the catalytic cycle (figure 1) cannot occur, thus the catalytic cycle will not proceed. This will prevent binding of substrate to heme in step 7, and thus there will not be a catalytic peak and substrate will not be metabolized. This shows the importance of oxygen.

As can be seen from figures 34 through 40, the addition of fenbendazole to a hemin-containing solution causes a catalytic peak to appear, while the addition of ASA does not. This means that, for the setup used during this research, fenbendazole shows reactivity, while ASA seems to be completely inactive. A possible explanation is that the conditions used were suboptimal for ASA, which led to there not being any reactivity despite being supposed to undergo the same metabolic pathway.

5. Conclusion

Hemin was found to be reduced at -0.361 V vs. Ag/AgCl in saturated KCl at 0.1 V/s, and adding pyridine brings this potential to -0.322 V vs. Ag/AgCl in saturated KCl at 0.1 V/s. Due to a shift in $E_{1/2}$ when adding pyridine, it is suggested that pyridine binds to hemin, thus forming a penta-coordinated molecule which, after reduction of Fe^{3+} into Fe^{2+}, can also transform from a low-spin to a high-spin molecule. This allows the catalytic cycle to occur.

A linear relationship is seen between I_P and √v for all experiments with hemin, indicating a diffusion-controlled system, however there is an indication of electrode-adsorption of hemin. In this system, adding fenbendazole showed reactivity, but ASA did not show reactivity. This reactivity indicates presence and absence of metabolism respectively, and it is suggested that this difference is caused by the conditions of the experiments, which might be suboptimal for ASA. By presence of some reactivity, it can be concluded that it is possible to use hemin as a catalyst for drug metabolism, but not all drugs are viable candidates for this type of metabolite research. In order to find out more about which drugs are viable candidates for this type of research, a follow-up study can first be done in order to determine which chemical properties of drugs are important which allow metabolism by CYP and hemin, and what the optimal test conditions are for each drug prior to practical work.

6. References

1. Xu C, Li CYT, Kong ANT. Induction of phase I, II and III drug metabolism/transport by xenobiotics. Arch Pharm Res. 2005 Mar;28(3):249–68.
2. Dang N le, Matlock MK, Hughes TB, Swamidass SJ. The Metabolic Rainbow: Deep Learning Phase I Metabolism in Five Colors. J Chem Inf Model. 2020 Mar 23;60(3):1146–64.
3. Williams JA, Hyland R, Jones BC, Smith DA, Hurst S, Goosen TC, et al. DRUG-DRUG INTERACTIONS FOR UDP-GLUCURONOSYLTRANSFERASE SUBSTRATES: A PHARMACOKINETIC EXPLANATION FOR TYPICALLY OBSERVED LOW EXPOSURE (AUC $_{i}$ /AUC) RATIOS. Drug Metabolism and Disposition. 2004 Nov;32(11):1201–8.
4. Liu Y, Wu X, Lv H, Cao Y, Ren H. Boosting the photocatalytic hydrogen evolution activity of g-C $_{3}$ N $_{4}$ nanosheets by Cu $_{2}$ (OH) $_{2}$ CO $_{3}$ -modification and dye-sensitization. Dalton Transactions. 2019;48(4):1217–25.
5. Das DK, Bhattaray C, Medhi OK. Electrochemical behaviour of (protoporphyrinato IX)iron(III) encapsulated in aqueous surfactant micelles. Journal of the Chemical Society, Dalton Transactions. 1997;(24):4713–8.
6. Graham DJ. Standard Operating Procedures for Cyclic Voltammetry. 2018.
7. Elgrishi N, Rountree KJ, McCarthy BD, Rountree ES, Eisenhart TT, Dempsey JL. A Practical Beginner's Guide to Cyclic Voltammetry. J Chem Educ. 2018 Feb 13;95(2):197–206.
8. Carroll KM, Knoll AW, Wolf H, Duerig U. Explaining the Transition from Diffusion Limited to Reaction Limited Surface Assembly of Molecular Species through Spatial Variations. Langmuir. 2018 Jan 9;34(1):73–80.
9. Konopka SJ, McDuffie Bruce. Diffusion coefficients of ferri- and ferrocyanide ions in aqueous media, using twin-electrode thin-layer electrochemistry. Anal Chem. 1970 Dec 1;42(14):1741–6.

10. US Government. National Institute of Standards and Technology. Engineering Statistics Handbook. National Institute of Standards and Technology.

11. Lenga RE. The Sigma-Aldrich library of chemical safety data. 1988.

12. Groot MTDe. Electrochemistry of immobilized heme and heme proteins. Eindhoven; 2007.

13. Liu G, Zhang H, Liu G, Yuan S, Liu C. Tetraalkylammonium interactions with dodecyl sulfate micelles: a molecular dynamics study. Physical Chemistry Chemical Physics. 2016;18(2):878–85.

14. Compton DL. Bioelectrocatalytic Reactions in Room-Temperature Ionic Liquids. ECS Proceedings Volumes. 2002 Jan;2002–19(1):234–43.

15. Vashi PR, Marques HM. The coordination of imidazole and substituted pyridines by the hemeoctapeptide N-acetyl-ferromicroperoxidase-8 (FeIINAcMP8). J Inorg Biochem. 2004 Sep;98(9):1471–82.

16. Boniolo M, Shylin SI, Chernev P, Cheah MH, Heizmann PA, Huang P, et al. Spin transition in a ferrous chloride complex supported by a pentapyridine ligand. Chemical Communications. 2020;56(18):2703–6.

17. Shikama K. Nature of the FeO2 bonding in myoglobin and hemoglobin: A new molecular paradigm. Prog Biophys Mol Biol. 2006 May;91(1–2):83–162.

18. Pieter. We make images, of molecules. Studio Molekuul.

7. Appendix

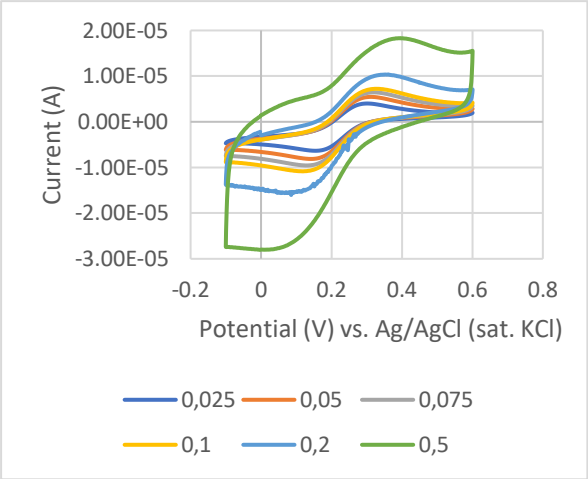

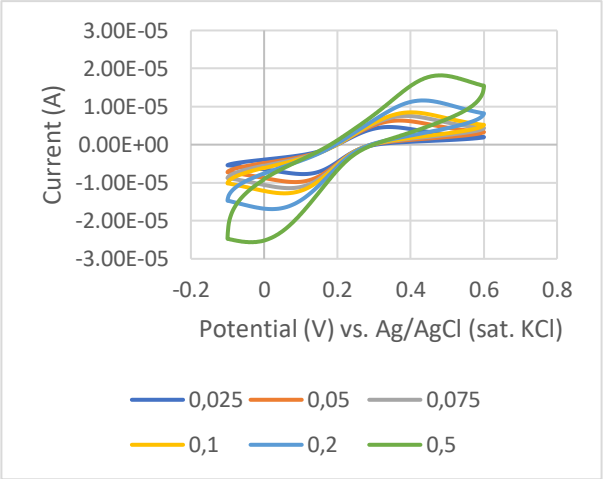

Figures A1 and A2: Voltammograms showing the relation between I_P and v

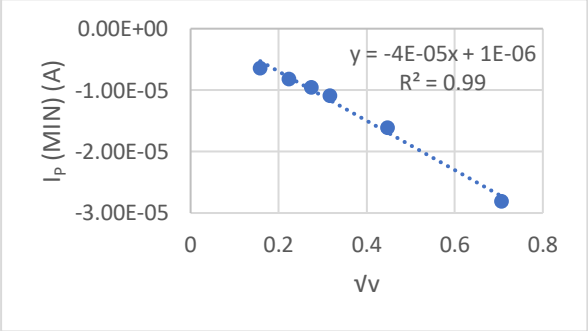

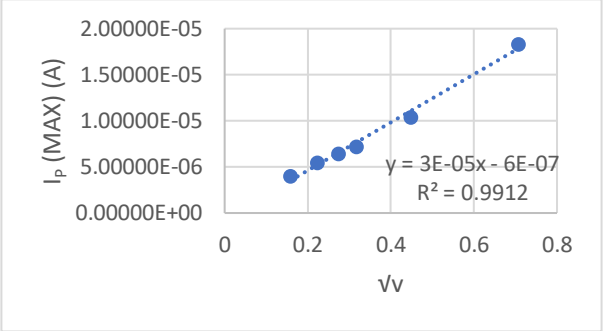

Figures A3 and A4: Reduction of ferricyanide (left) and oxidation of ferrocyanide (right) for figure A1

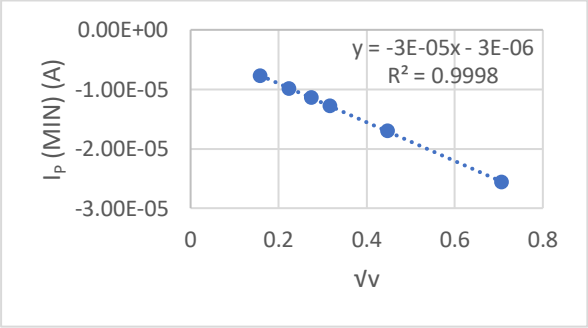

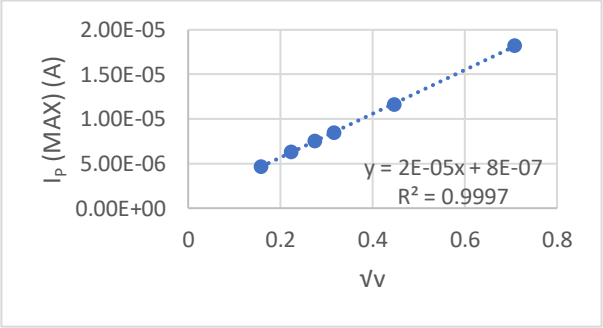

Figures A5 and A6: Reduction of ferricyanide (left) and oxidation of ferrocyanide (right) for figure A2

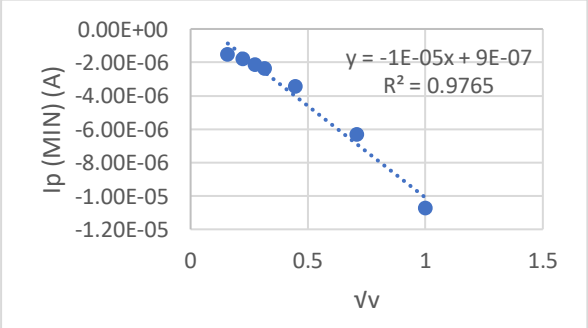

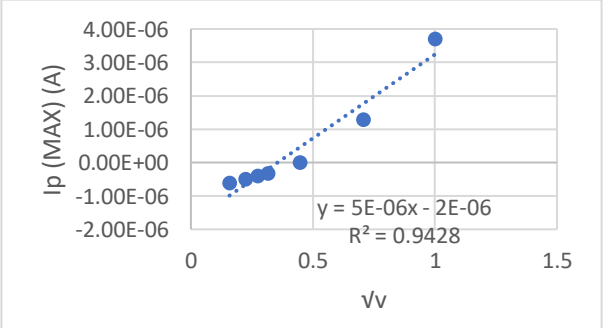

Figures B1 and B2: Reduction of hemin (left) and reoxidation of hemin (right) for data H1 in figure 15

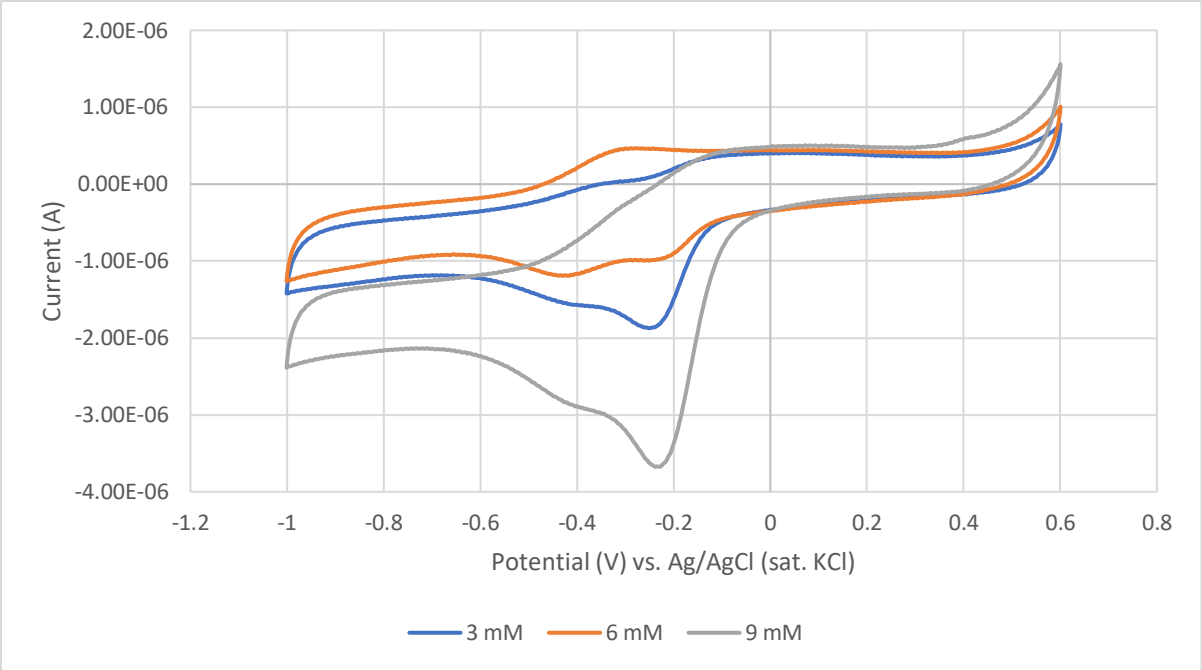

Figure C1: Hemin concentration study